Consequences of Replacing the DNA 3′-Oxygen by an Amino Group: High-Resolution Crystal Structure of a Fully Modified N3′ → P5′ Phosphoramidate DNA Dodecamer Duplex†

Valentina Tereshko,‡ Sergei Gryaznov,§ and Martin Egli*,‡

Contribution from the Drug Discovery Program and Department of Molecular Pharmacology and Biological Chemistry, Northwestern University Medical School, 303 East Chicago Avenue, Chicago, Illinois 60611-3008, and Lynx Therapeutics Inc., 3832 Bay Center Place, Hayward, California 94545

Received June 13, 1997⊗

Abstract: As part of the quest for antisense compounds with relative to DNA and RNA improved nuclease-resistance and favorable RNA hybridization properties, a large variety of oligonucleotide analogues has been generated in recent years. Among these, the oligonucleotide N3′ → P5′ phosphoramidate DNA (3′-NP DNA), an analogue with the 3′-oxygen in the nucleic acid sugar−phosphodiester backbone replaced by an amino group, displays several unique features. Self-pairing of 3′-NP DNA single strands is significantly favored thermodynamically over self-pairing of both DNA and RNA (Gryaznov, S. M.; et al. *Proc. Natl. Acad. Sci. U.S.A.* **1995**, *92*, 5798−5802). CD measurements in solution have shown that the duplex conformation of 3′-NP DNA is very similar to the RNA A-form. Moreover, 3′-NP DNA can form stable triplexes with double-stranded DNA under conditions where native DNA fails to do so. Recently, it was shown that all-phosphoramidate DNA analogues of HIV-1 RRE and TAR RNA specifically bind to the RNA-binding Rev- and Tat-related peptides (Rigl, C. T.; et al. *Biochemistry* **1997**, *36*, 650−659). We have determined the X-ray crystal structure of the all-modified 3′-NP DNA duplex $[5'\text{-d(CnpGnpCnpGnpAnpAnpTnpTnpCnpGnpCnpG)}]_2$ at 2-Å resolution. Whereas the Dickerson−Drew type phosphodiester DNA 5′-d(CGCGAATTCGCG) adopts a B-form duplex in the crystal as well as in solution, the 3′-NP DNA duplex with identical sequence displays an A-RNA conformation in the crystal. Combined with the earlier CD results in solution, our observation provides convincing evidence that the A-conformation with 3′-NP DNA is modification- and not sequence-induced. The crystal structure reveals a dramatically improved hydration of the phosphoramidate DNA relative to DNA due to the presence of the amino group in its sugar−phosphate backbone. Compared with A-DNA and A-RNA, the 3′-NP DNA duplex geometry appears more uniform, with backbone torsion angles of individual nucleotides displaying only minor variations. This is consistent with an observed repetitive pattern of coordination by either chloride anions or water molecules to the 3′-amino groups in the crystal, suggesting a strong anomeric effect between the 3′-nitrogen lone electron pair and the σ^* orbital of the P−O5′ bond. Our crystal structure can qualitatively explain the exceptional thermodynamic stability of 3′-NP DNA, and helps to rationalize previously ill understood findings, such as the surprising fact that DNA with NH substituted for O5′ fails to pair with either DNA or RNA. The crystal structure also establishes 3′-NP DNA as the quintessential RNA mimetic, in terms of overall duplex structure, rigidity, and level of hydration.

The concept to inhibit protein synthesis through interfering with biological information transfer at various stages,[1] by sequence-specific binding of an oligonucleotide to either single-stranded RNA or double-stranded DNA (antisense and antigene approach, respectively),[2] is currently widely being tested for its therapeutic potential in the treatment of diseases including cancer, AIDS, and inflammation.[3] The fact that native DNA and RNA are not enough resistant to nucleolytic degradation has stimulated an extensive search for chemical modifications that would provide the oligonucleotide with sufficient metabolic stability, while retaining or improving its ability to bind to a complementary target with high affinity and sequence specificity. Most of the modification sites of first- and second-generation antisense oligonucleotides concern the atoms of the sugar−phosphate backbone as well as the bases within the framework of natural DNA and RNA.[4] However, some

* Corresponding author: Phone (312) 503-0845; Fax (312) 503-0796; E-mail m-egli@nwu.edu.

† Coordinates deposited in the Nucleic Acid Data Base, entry code ADLS105.

‡ Northwestern University Medical School.

§ Lynx Therapeutics Inc.

⊗ Abstract published in *Advance ACS Abstracts,* December 15, 1997.

(1) (a) Zamecnik, P. C.; Stephenson, M. L. *Proc. Natl. Acad. Sci. U.S.A.* **1978**, *75*, 280−284. (b) Stephenson, M. L.; Zamecnik, P. C. *Proc. Natl. Acad. Sci. U.S.A.* **1978**, *75*, 285−288.

(2) (a) Uhlmann, E.; Peyman, A. *Chem. Rev. (Washington, D.C.)* **1990**, *90*, 543−584. (b) Milligan, J. F.; Matteucci, M. D.; Martin, J. C. *J. Med. Chem.* **1993**, *36*, 1923−1937. (c) *Antisense Research and Applications*; Crooke, S. T., Lebleu, B., Eds.; CRC Press: Inc., Boca Raton, FL, 1993. (d) Altmann, K.-H.; Dean, N. M.; Fabbro, D.; Freier, S. M.; Geiger, T.; Häner, R.; Hüsken, D.; Martin, P.; Monia, B. P.; Müller, M.; Natt, F.; Nicklin, P.; Phillips, J.; Pieles, U.; Sasmor, H.; Moser, H. E. *Chimia* **1996**, *50*, 168−176.

(3) (a) Narayanan, R.; Akhtar, S. *Curr. Opin. Oncol.* **1996**, *8*, 509−515 and references cited therein. (b) Szymkowski, D. E. *Drug Discov. Today* **1996**, *1*, 415−428 and references cited therein. (c) Akhtar, S.; Agrawal, S. *Trends Pharmacol. Sci.* **1997**, *18*, 12−19 and references cited therein. (d) Nyce, J. W.; Metzger, W. J. *Nature* **1997**, *385*, 721−725.

S0002-7863(97)01962-8 CCC: $15.00
Published on Web 01/01/1998

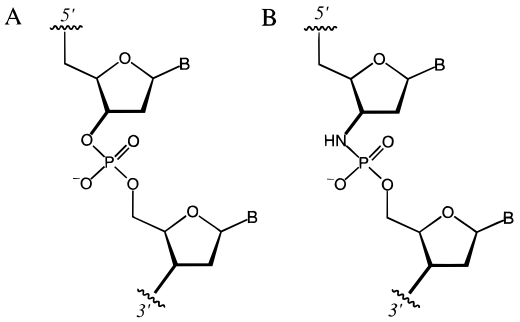

Figure 1. Structure of (A) DNA and (B) 3′-NP DNA.

analogue designs deviate more drastically from the natural backbone[5] or base structures.[6] While most studies characterizing these oligonucleotide analogues have been concerned with an assessment of the effects of the modifications on nuclease resistance and DNA- or RNA-binding affinities, only a few modifications have been subjected to a detailed structural characterization in the oligonucleotide context.[7,8] Using single-crystal X-ray crystallography, we are studying the effects of a large variety of modifications on DNA and RNA duplex structure and hydration. It is hoped that the elucidation of precise three-dimensional structures of modified nucleic acids and their correlation with available thermodynamic data will not only further our understanding of nucleic acid structure in general, but will eventually be of help in the design of improved second- and third-generation nucleic acid analogues for therapeutic applications.

The synthesis of N3′ → P5′ phosphoramidate DNA oligonucleotides has recently been reported.[9] The N3′ → P5′ phosphoramidate DNA (3′-NP DNA) contains an achiral 3′-NHP(O)(O$^-$)O-5′ internucleoside linkage in place of the 3′-OP(O)(O$^-$)O-5′ phosphodiester linkage in natural DNA (Figure 1). 3′-NP DNA oligonucleotides display improved nuclease resistance in comparison with the natural phosphodiester compounds.[9,10] Evaluation of the hybridization properties of 3′-NP DNA oligonucleotides to complementary DNA and RNA strands showed an enhancement of the duplex thermal stability by 2.3−2.6 °C per linkage relative to the phosphodiester compounds, independent of nucleotide sequence and base composition.[9,10] Oligonucleotides with alternating phosphodiester−phosphoramidate linkages were also found to bind more tightly to the RNA complement compared with the corresponding DNA, but formed less stable complexes with the DNA complement than their DNA counterpart.[9,10] 3′-NP DNA forms considerably more stable duplexes with itself than isosequential DNA and RNA strands. Another interesting property of 3′-NP DNA is its capability to form stable triplexes (as the third homopyrimidine strand) with both double-stranded DNA and RNA under neutral pH conditions, where triplex formation with a phosphodiester third strand is not observed.[9,10] In addition, while pyrimidine DNA oligonucleotides cannot form stable triplexes with heteroduplexes where the homo-purine strand is RNA,[11] RNA can, and likewise, 3′-NP DNA was observed to produce stable triplexes as well. This is consistent with CD experiments that point to a conformation of double-helical 3′-NP DNA similar to the RNA A-form,[10] and 2-dimensional NMR data that suggest adoption of predominantly N-type sugar puckering by the furanose rings of 3′-aminonucleotides in 3′-NP DNA duplexes.[12]

Its relatively high resistance to nucleases as well as its favorable hybridization and triplex-formation properties render 3′-NP DNA a promising candidate for antisense and antigene applications. Indeed, in vitro, uniformly modified 3′-NP DNA oligonucleotides are apparently more potent antisense agents than phosphorothioate derivatives. A recent investigation of the antileukemia effect of *c-myc* 3′-NP DNA oligonucleotides in vivo suggests that phosphoramidates can serve as potent and specific antisense agents in the treatment of human leukemia and potentially of other malignancies as well.[13] Although heteroduplexes between uniformly modified 3′-NP DNA oligonucleotides and complementary RNA are not recognized as substrates by RNaseH, only the uniformly modified phosphoramidate oligonucleotide targeted against the human T cell leukemia virus type I−Tax protein caused a sequence-dependent reduction in the Tax protein level, whereas neither the chimeric phosphodiester−phosphoramidate nor the corresponding phosphorothioate oligonucleotides led to any significant reduction of protein expression.[14] This strongly suggests an RNase H-independent antisense activity of 3′-NP DNA, most likely related to its stable hybridization with RNA. As a consequence of the stable triplex formation of 3′-NP DNA with double-stranded DNA targets, efficient inhibition of transcription elongation in vitro was observed with phosphoramidate oligonucleotides targeted to proviral HIV DNA.[15] In a recent study, it was demonstrated that a 3′-NP DNA oligonucleotide can recognize and specifically bind to a 15-base-pair sequence within the chromatin structure of cell nuclei.[16] A most remarkable finding, considering the fact that 3′-NP DNA is composed of modified 2′-deoxynucleotides, is the observation that 3′-NP DNA analogues of the HIV-1 RRE and TAR elements, both rich in noncanonical secondary structure, bound specifically to Rev- and Tat-related peptides, notably with affinities that were only insignificantly reduced compared with the natural RNA substrates.[17]

(4) (a) Varma, R. S. *Synlett* **1993**, 621−637. (b) De Mesmaeker, A.; Häner, R.; Martin, P.; Moser, H. E. *Acc. Chem. Res*. **1995**, *28*, 366−374. (c) De Mesmaeker, A.; Altmann, K.-H.; Waldner, A.; Wendeborn, S. *Curr. Opin. Struct. Biol*. **1995**, *5*, 343−355.

(5) Among phosphate backbone surrogates, e.g.: (a) (peptide nucleic acids (PNAs)): Nielsen, P. E.; Egholm, M.; Buchardt, O. *Bioconjugate Chem.* **1994**, *5*, 3−7. Eriksson, M.; Nielsen, P. E. *Q. Rev. Biophys.* **1996**, *29*, 369−394 and references cited therein. (b) (amide linkers) De Mesmaeker, A.; Waldner, A.; Lebreton, J.; Hoffmann, P.; Fritsch, V.; Wolf, R. M.; Freier, S. M. *Angew. Chem., Int. Ed. Engl.* **1994**, *33*, 226−229. (c) (guanidine linkers) Dempcy, R. O.; Browne, K. A.; Bruice, T. C. *Proc. Natl. Acad. Sci. U.S.A.* **92**, 6097−6101.

(6) Among base pair surrogates, e.g.: (a) (phenoxazine) Lin, K.-Y.; Jones, R. J.; Matteucci, M. *J. Am. Chem. Soc.* **1995**, *117*, 3873−3874. (b) (stilbenedicarboxamide bridges) Letsinger, R. L.; Wu, T. *J. Am. Chem. Soc.* **1995**, *117*, 7323−7328.

(7) Portmann, S.; Altmann, K.-H.; Reynes, N.; Egli, M. *J. Am. Chem. Soc.* **1997**, *119*, 2396−2403 and references cited therein.

(8) Some recent X-ray crystal structure determinations of chemically modified di- and oligonucleotide fragments have been reviewed: Egli, M. *Angew. Chem., Int. Ed. Engl.* **1996**, *35*, 1894−1909.

(9) (a) Gryaznov, S. M.; Chen, J.-K. *J. Am. Chem. Soc.* **1994**, *116*, 3143−3144. (b) Chen, J.-K.; Schultz, R. G.; Lloyd, D. H.; Gryaznov, S. M. *Nucleic Acids Res.* **1995**, *23*, 2661−2668.

(10) Gryaznov, S. M.; Lloyd, D. H.; Chen, J.-H., Schultz, R. G.; DeDionisio, L. A.; Ratmeyer, L.; Wilson, W. D. *Proc. Natl. Acad. Sci. U.S.A.* **1995**, *92*, 5798−5802.

(11) (a) Roberts, R. W.; Crothers, D. M. *Science* **1992**, *258*, 1463−1466. (b) Hau, H.; Dervan, P. B. *Proc. Natl. Acad. Sci. U.S.A.* **1993**, *90*, 3806−3810.

(12) Ding, D.; Gryaznov, S. M.; Lloyd, D. H.; Chandrasekaran, S.; Yao, S.; Ratmeyer, L.; Pan, Y.; Wilson, W. D. *Nucleic Acids Res.* **1996**, *24*, 354−360.

(13) Skorski, T.; Perrotti, D.; Nieborowska-Skorski, M.; Gryaznov, S.; Calabretta, B. *Proc. Natl. Acad. Sci. U.S.A.* **1997**, *94*, 3966−3971.

(14) Heidenreich, O.; Gryaznov, S.; Nerenberg, M. *Nucleic Acids Res.* **1997**, *25*, 776−780.

(15) Giovannangeli, C.; Perrouault, L.; Escudé, C.; Gryaznov, S.; Hélène, C. *J. Mol. Biol.* **1996**, *261*, 386-398.

(16) Giovannangeli, C.; Diviacco, S.; Labrousse, V.; Gryaznov, S.; Charneau, P.; Hélène, C. *Proc. Natl. Acad. Sci. U.S.A.* **1997**, *94*, 79−84.

Several unexpected findings with 3′-NP DNA warrant a detailed investigation of their origins. Thus, a conclusion one might have drawn from the accumulated thermodynamic stability data of hybridizations between modified nucleic acids and RNA is that RNA analogues will in general pair more strongly with RNA than do DNA analogues. Therefore, it is surprising that 3′-NP DNA as a DNA analogue not only displays an exceptionally high affinity for RNA, but surpasses most other nucleic acid-based pairing systems in terms of the stability of its self-pairing.[18] At this point, one may mention that probably not very many people, even among those intimately familiar with modified nucleic acids, would have predicted the observed substantial stability gains as a consequence of the relatively "modest" chemical alteration of the sugar−phosphate backbone in 3′-NP DNA. Further, relative to isosequential phosphodiester oligomers, oligo-2′-fluoro-2′-deoxy N3′ → P5′ phosphoramidates display melting temperatures of their duplexes with DNA or RNA that are increased by ca. 4 or 5 °C per modification, respectively.[19] Conversely, oligonucleotide N3′ → P5′ phosphoramidates containing a single 3′-amino-2′-methoxy substitution form significantly less stable duplexes with RNA and DNA strands than do all-2′-deoxy-N3′ → P5′ phosphoramidates.[20] However, their 2′-methoxy phosphodiester counterparts form duplexes with RNA that normally surpass the stability of the corresponding DNA−RNA hybrids by around 1 °C per modification.[21] Another puzzling observation is the fact that *N*5′-phosphoramidates containing 3′-O(O$^-$)(O)PNH-5′ internucleoside linkages pair with neither DNA nor RNA.[10] In a recent computational simulation study, hydration effects have been invoked to explain the differences between the pairing properties of 3′- and 5′-phosphoramidates.[22]

To shed light on structural features of 3′-NP DNA that might explain several or all of its surprising pairing and functional properties, we have determined the crystal structure of the fully modified 3′-NP DNA duplex with sequence 5′-d(CnpGnpCnpGnpAnpAnpTnpTnpCnpGnpCnpG) (np is the abbreviation for the 3′-NHP(O)(O$^-$)O-5′ phosphoramidate linkage) at 2-Å resolution. It constitutes the first crystal structure of an all-chemically-modified DNA double helix.[23] Its sequence is identical with the one of the so-called Dickerson−Drew dodecamer that constitutes the first B-form DNA duplex whose structure was solved by X-ray crystallography.[24] Since then, 40 crystal structures of DNA duplexes with the same sequence or variations thereof have been determined, either DNA-only or complexed with a variety of minor groove binding drugs,[25] all essentially exhibiting only minor deviations from the B-form genus of the original structure. By choosing this sequence, we can be quite confident that all conformational alterations that might be observed in the structure of the 3′-NP DNA dodecamer relative to the native B-DNA can be attributed to the 3′-amino modification in the backbone of the phosphoramidate strand. Here, we report the crystallization and structure determination of the 3′-NP DNA duplex as well as the conformational and geometrical details of the double helix. The overall duplex structure adopted by 3′-NP DNA resembles that of the RNA A-form, and the 3′-amino moiety in its backbone is found to confer a large number of water molecules on both backbone and groove sites. In addition, hydrogen bonding interactions between the 3′-amino groups and chloride anions as well as water molecules in the crystal result in a strong anomeric effect between the 3′-nitrogen lone pair and the antibonding σ^* orbital from the adjacent P−O5′ bond, the conjugation causing a considerably reduced flexibility of the 3′-NP DNA duplex backbones in comparison with both A-form DNA and RNA.

Materials and Methods

Oligonucleotide Synthesis and Purification. The dodecamer 5′-d(CnpGnpCnpGnpAnpAnpTnpTnpCnpGnpCnpG) was synthesized on a 400 μmol scale on an ABI 390Z synthesizer, using the previously described protocols for assembly of 3′-NP DNA oligonucleotides.[9] After deprotection, the oligonucleotide was purified by ion exchange HPLC as described in ref 9b. The oligonucleotide was desalted on a NAP10 column (Pharmacia) and then lyophilized. Purity was ≥95%.

Crystallization. The concentration of the oligonucleotide was adjusted to 10 mM (single strand) in water. Initial crystallization experiments were performed with the sitting drop vapor diffusion method, equilibrating droplets with 1.5 mM phosphoramidate dodecamer, 40 mM sodium cacodylate buffer (pH 6.9−7.4), $MgCl_2$ or $CaCl_2$ (10−500 mM), and spermine tetrahydrochloride (1−30 mM) against a reservoir of 20−40% 2-methyl-2,4-pentanediol (MPD). In general, such conditions produced thin triangular crystals which diffracted only to low resolution, with diffraction restricted to two dimensions. Since these typical nucleic acid crystallization conditions did not produce any useful crystals, we resorted to several commercially available protein and nucleic acid sparse matrix crystallization screens. Screening solutions with pH values below 6.5 were rejected since the phosphoramidates are chemically unstable at pH ≤ 6. The only crystals suitable for a high-resolution structure were obtained with solution 33 of the NATRIX crystal sceen kit (Hampton Research). In a typical crystallization experiment at 20 °C, 5 μL hanging droplets with 1 mM phosphoramidate, 100 mM ammonium chloride, 5 mM $MgCl_2$, 25 mM Na Hepes, pH 7.0, and 15% 1,6-hexanediol were equilibrated against a 0.5 mL reservoir, containing 200 mM ammonium chloride, 10 mM $MgCl_2$, 50 mM Na Hepes, pH 7.0, and 30% 1,6-hexanediol. Thick needles with typical dimensions 0.15 × 0.15 × 0.6 mm appeared after as early as one week, but occasionally grew after as long as one month.

(17) Rigl, C. T.; Lloyd, D. H.; Tsou, D. S.; Gryaznov, S.; Wilson, W. D. *Biochemistry* **1997**, *36*, 650−659.

(18) (a) Most, but not all: e.g., pyranosyl-RNA (p-RNA) self-pairing is of similar stability. Under similar experimental conditions (10 μM nucleic acid, Tris·HCl pH 7, 0.15 M NaCl), the UV-melting temperatures of the p-RNA and 3′-NP DNA duplexes with sequence $(A)_{10}/(T)_{10}$ are 40 and 43 °C, respectively. However, p-RNA pairs only weakly with RNA. For recent publications on the pairing and structural properties of p-RNA, see: Pitsch, S.; Wendeborn, S.; Jaun, B.; Eschenmoser, A. *Helv. Chim. Acta* **1993**, *76*, 2161−2183. Pitsch, S.; Krishnamurthy, R.; Bolli, M.; Wendeborn, S.; Holzner, A.; Minton, M.; Lesueur, C.; Schlönvogt, I.; Jaun, B.; Eschenmoser, A. *Helv. Chim. Acta* **1995**, *78*, 1621−1635. Krishnamurthy, R.; Pitsch, S.; Minton, M.; Miculka, C.; Windhab, N.; Eschenmoser, A. *Angew. Chem., Int. Ed. Engl.* **1996**, *35*, 1537−1541. Schlönvogt, I.; Pitsch, S.; Lesueur, C.; Eschenmoser, A.; Jaun, B.; Wolf, R, M. *Helv. Chim. Acta* **1996**, *79*, 2316−2345. (b) Other strongly stabilizing modifications are 2′-*O*-(methoxyethyl)-RNA (see ref 2d) and 2′-fluoro-DNA: Kawasaki, A. M.; Casper, M. D.; Freier, S. M.; Lesnik, E. A.; Zounes, M. C.; Cummins, L. L.; Gonzalez, C.; Cook, P. D. *J. Med. Chem.* **1993**, *36*, 831−841.

(19) Schultz, R. G.; Gryaznov, S. M. *Nucleic Acids Res.* **1996**, *24*, 2966−2973.

(20) Gryaznov, S. Unpublished results.

(21) (a) Inoue, H.; Hayase, Y.; Imura, A.; Iwai, S.; Miura, K.; Ohtsuka, E. *Nucleic Acids Res.* **1987**, *15*, 6131−6148. (b) Iribarren, A. M.; Sproat, B. S.; Neuner, P.; Sulston, I.; Ryder, U.; Lamond, A. I. *Proc. Natl. Acad. Sci. U.S.A.* **1990**, *87*, 7747−7751. (c) Lesnik, E. A.; Guinosso, C. J.; Kawasaki, A. M.; Sasmor, H.; Zounes, M.; Cummins, L. L.; Ecker, D. J.; Cook, P. D.; Freier, S. M. *Biochemistry* **1993**, *32*, 7832−7838.

(22) Barsky, D.; Colvin, M. E.; Zon, G.; Gryaznov, S. M. *Nucleic Acids Res.* **1997**, *25*, 830−835.

(23) The crystal structure of an all-PNA double helix has recently been reported: Rasmussen, H.; Kastrup, J. S.; Nielsen, J. N.; Nielsen, J. M.; Nielsen, P. E. *Nature Struct. Biol.* **1997**, *4*, 98−101.

(24) (a) Wing, R.; Drew, H.; Takano, T.; Broka, C.; Tanaka, S.; Itakura, K.; Dickerson, R. E. *Nature* **1980**, *287*, 755−758. (b) Dickerson, R. E.; Drew, H. R. *J. Mol. Biol.* **1981**, *149*, 761−786.

(25) Kopka, M. L.; Larsen, T. A. Netropsin and the Lexitropins. The Search for Sequence-Specific Minor-Groove-Binding Ligands. In *Nucleic Acid Targeted Drug Design*; Probst, C. L., Perun, T. J., Eds.; Marcel Dekker, Inc.: New York, 1992; pp 303−374.

Table 1. Selected Crystal Data, X-ray Data Collection Parameters and Merging Statistics

parameter	5′-d(CnpGnpCnpGnpAnpAnpTnpTnpCnpGnpCnpG)	
	Crystal Data	
a (Å)	40.15	
b (Å)	40.15	
c (Å)	304.21	
V (Å^3)	424,693.1	
space group[a]	*R*32	*R*3
asymmetric unit[b]	36 base pairs or 3 duplexes, each 50% occupied	72 base pairs, or 6 duplexes, each 50% occupied
V/base pair (Å^3)	1310.8	
	Data Collection and Processing	
temperature	RT	
resolution (Å)	34−2.0	34−2.0
collected reflections	76 542	76 542
unique reflections	6,737	11,835
completeness (whole range, %)	98.4	96.2
R_{merge}[c] (all reflections, %)	8.2	7.9

[a] The structure was solved in the lower symmetry space group (*R*3), and data for both space groups are therefore given. [b] In the lattice, the crystallographic 2-fold rotation axes of space group *R*32 do not coincide with any of the molecular 2-fold rotation axes of dodecamer duplexes in the stack. The lattice can be thought of as composed of alternating infinite stacks of helixes that are shifted by exactly one base pair step relative to one another. The crystal is thus a precise twin, composed of 50% of one type of helix stack and 50% of the other. The asymmetric unit of the *R*3 lattice is a superposition of two helix stacks, containing three duplexes each, thus corresponding to a total of 2916 DNA atoms with occupancy 0.5. This arrangement generates a crystallographic 2-fold rotation axis which runs through the sixth base pair of the middle duplex, resulting in effective *R*32 symmetry of the crystal (Figure 2). The 2-fold axis relates the bottom 1.5 duplexes of one stack to the top 1.5 of the other, the asymmetric unit of *R*32 thus consisting of a total of three duplexes with 1458 atoms, each with occupancy 0.5. [c] $R_{merge} = \Sigma(I - \langle I \rangle)^2/\Sigma I$,[2] where $\langle I \rangle$ is the average intensity of a particular reflection. It provides a measure for the agreement between symmetry-related reflections.

Varying these initial conditions revealed that ammonium chloride in relatively high concentrations was absolutely required for crystal growth. Replacing it with either sodium or potassium chloride did not produce any crystals.

Crystallographic Data Collection. A fragment with size 0.3 × 0.3 × 0.3 mm of a larger crystal was sealed in a capillary with a droplet of mother liquor and mounted on a Rigaku R-AXIS-II image plate/rotating anode X-ray generator system. The detector−crystal distance was set to 120 mm, and the detector was swung out to 10° (2θ angle). Two sets of frames were measured with exposure times of 5 and 10 min, respectively (80 frames each, with an oscillation angle of 1.5°). Data were processed with the DENZO/SCALEPACK[26] program package in the rhombohedral space groups *R*3 and *R*32 (hexagonal setting), and the resulting R_{merge} values were very similar. Selected crystal data, X-ray data collection parameters, and merging statistics are listed in Table 1. To extend the resolution of the data beyond 2 Å, several attempts were undertaken to collect data at low temperature. Conditioning the crystals and then shock-freezing them to −170 °C in a nitrogen gas stream generally led to lower quality data due to higher mosaicity, without significantly improving the resolution (typically around 1.85−1.90 Å). The entire analysis of the phosphoramidate duplex crystal structure was therefore carried out with data collected at room temperature.

Structure Solution and Refinement. The overall unit cell dimensions of the phosphoramidate duplex crystal, *a* and *b* around 40 Å, combined with a much longer *c* cell constant, were somewhat reminiscent of the cell dimensions of an RNA octamer duplex whose struture we had determined two years ago.[27] The space group of the RNA crystals was *R*32 (cell parameters $a = b = 42.7$ Å, $c = 131.7$ Å), and in that lattice adjacent RNA duplexes were stacked, generating infinite helixes along the 3-fold screw axes. The duplexes in the RNA crystal assumed general orientations; thus, molecular 2-fold rotation axes did not coincide with either of the two classes of crystallographic 2-folds present in space group *R*32. The *c*-cell constant was thus determined by the length requirements of six stacked octamer duplexes. On the basis of this spatial arrangement, the helical rise of the RNA duplex was deduced to be ca. 2.75 Å. With this in mind, the unit cell of the phosphoramidate crystals was thought to contain 27 dodecamer duplexes (hexagonal setting), the *R*32 asymmetric unit consisting of 1.5 duplexes. Inspection of the Patterson maps had previously revealed continuous stacking along the *z*-axis in the phosphoramidate dodecamer lattice. Therefore, the *c*-cell constant would correspond to the long dimension of a stack of nine duplexes. This meant an average helical rise per base pair step of ca. 2.8 Å, consistent with an A-form duplex. In space group *R*32 there are two classes of 2-fold rotation axes which are separated by 1/6 in the direction of the *z*-axis. Therefore, either class of crystallographic 2-folds could be intramolecular and thus coincide with the molecular 2-fold axis of every other dodecamer duplex in the infinite stacks. Rotation/translation searches were carried out with program AMORE[28] or by shifting an A-form duplex along both classes of crystallographic 2-folds, followed by difference Fourier synthesis in order to locate the second duplex. However, all attempts to locate and refine the position of the duplex on the 2-fold rotation axis were futile.

Further searches were then performed in the lower symmetry space group *R*3 (the asymmetric unit in *R*3 consists of three duplexes; see Table 1). Using the molecular replacement program AMORE and an A-form model with helical rise 2.8 Å and 11 residues per turn, a rotation and three-body translation search was conducted. With this approach, six best solutions were established; further solutions were characterized by markedly lower correlation coefficients and higher *R*-values. The best solutions correspond to two different stacks composed of three duplexes (solutions 1 and 2, Table 2), the stacks being shifted and rotated relative to one another by roughly 2.8 Å and 30°, respectively. As in the A-RNA crystals mentioned above, the duplexes are centered roughly on the 3-fold screw axis. Selected data for structure solution and refinement are summarized in Table 2. The two solutions were refined individually, and numerous cycles of positional and *B*-factor refinement combined with simulated annealing cycles using X-PLOR[29] resulted in satisfactory figures of merit for both (Table 2). Twelve intense peaks which showed up in sum ($2F_o - F_c$) and difference (F_o

(26) (a) Otwinowski, Z. "Oscillation Data Reduction Program. *Proceedings of the CCP4 Study Weekend: "Data Collection and Processsing*", Jan 29−30, 1993, compiled by L. Sawyer, N. Isaacs, and S. Bailey, SERC Daresbury Laboratory, England, pp 56−62. (b) Minor, W. XDISPLAYF Program, Purdue University, 1993.

(27) (a) Egli, M.; Portmann, S.; Tracz, D.; Workman, C.; Usman, N. *Acta Crystallogr., D* **1995**, *51*, 1065−1070. (b) Portmann, S.; Usman, N.; Egli, M. *Biochemistry* **1995**, *34*, 7569−7575.

(28) Navaza, J. *Acta Crystallogr., A* **1994**, *50*, 157−163.

(29) Refinement: (a) Brünger, A. T. 1992 *X-PLOR, A System for X-ray Crystallography and NMR (Version 3.1)*, Yale University Press: New Haven, CT. R_{free}: (b) Brünger, A. T. *Nature* **1992**, *355*, 472−475. (c) Kleywegt, G. J.; Brünger, A. T. *Structure* **1996**, *4*, 897−904.

Table 2. Structure Determination and Refinement Data

parameter	space group *R*32	space group *R*3
	Structure Determination	
rotation/translation search (8.0−2.5 Å)		solution 1: $R^a = 49.9\%$ (correlation coefficient 73.3%) solution 2: $R = 49.7\%$ (correlation coefficient 73.4%)
	Refinement Statistics	
resolution (Å)	8.0−2.0	
observed reflections[b]	5854	10 006
solution 1 (R, R_{free}[c] in %)		27.6, 33.8 (incl Cl^-)
solution 2 (R, R_{free}[c] in %)		27.8, 35.1 (incl Cl^-)
combination (1:1)	27.7, 32.1 (incl Cl^-)	
addition of more water molecules and ions, with *R*32 ncs-restraints (R, R_{free}[c] in %)	26.2, 29.1	
final *R*-factor[a,d] (%)	19.2	
final R_{free}[c,d] (%)	24.7	
DNA atoms	1458 (occup 0.5)	
solvent molecules and ions[e]	102 H_2O 6 Cl^- 12 NH_4^+	
average *B*-values of DNA atoms (Å^2)	18.8 ± 9.4	
average *B*-values of chloride ions (Å^2)	12.2 ± 2.3	
average *B*-values of ammonium ions (Å^2)	15.2 ± 1.0	
average *B*-values of water molecules (Å^2)	40.8 ± 10.7	
rms[f] deviation of bond lengths (Å)	0.010	
rms deviation of bond angles (deg)	1.35	
rms deviation of improper torsions (deg)	1.59	

[a] $R = \Sigma||F|_o - |F|_c|/\Sigma|F|_o$. [b] $F_o \geq 2\sigma(F_o)$ cutoff. [c] R_{free} is a cross-validation *R*-value for a test set of reflections[29] (10% for *R*32, 15% for *R*3). [d] Using the X-PLOR multiscale procedure, dividing the data into 10 separate bins. [e] Four of the water molecules have occupancy 0.5 (eight in *R*3). The chloride anions and ammonium cations are located on crystallographic 3-fold rotation axes and have occupancy 0.33. [f] rms = root mean square.

$- F_c$) Fourier maps were interpreted as chloride anions. The ions are located on 3-fold rotation axes between duplexes and lie roughly 3 Å from three backbone 3′-nitrogen atoms from symmetry-related duplexes. This interpretation is consistent with the important role ammonium chloride played in growing well-diffracting dodecamer crystals, and suggests that the ion-coordination mode is crucial for ordering phosphoramidate duplexes along the stacking direction.

What is the relation between the two solutions in terms of space group *R*32? The two duplex stacks are related by a crystallographic 2-fold rotation axis at $z = 1/6$. Thus, this crystallographic dyad is intramolecular (running through the middle duplex of three-duplex stacks, Figure 2A), and the dyads at $z = 0$ and $z = 1/3$ are intermolecular. However, a closer look at the stack revealed that the crystallographic (intramolecular) dyad does not coincide with the molecular one of the middle duplex, but instead runs through the sixth base pair, rotated by about 16° (half a helical twist) and translated by about 1.4 Å (half a helical rise) relative to the molecular dyad (Figure 2B, Table 1). The *R*32 asymmetric unit can be thought of as a superposition of two 18-base-pair duplexes (corresponding to 1.5 duplexes or half of the three-duplex stack), both with occupancy 0.5. In other words, the crystal is a merohedral perfect twin,[30] composed of stacks of duplexes both running along the *z*-axis, but displaced relative to one another by one base pair step (Figure 2A).

Clearly, the occurrence of such a peculiar packing arrangement is related to the intrinsic symmetry properties of the double helix, namely, the presence of two 2-fold rotation axes per base pair, one in the plane of each base pair and the other between every two adjacent base pairs (see Figure 1A in ref 31). In the present case, the local 2-fold in the plane of the sixth base pair (A·T) falls together with the crystallographic 2-fold (Figure 2B). The above 2-folds in and between base pair planes are only local but not global (molecular) 2-folds. Thus, rotation around them will result in more or less superimposed backbone atoms (Figures 2A and 3A). However, while the alignment of individual base pair planes is maintained upon rotation around a local 2-fold, the nature of the bases will not be restored in many cases, the actual number of occurrences depending on the specific sequence (Figure 2B). For example, rotation around the crystallographic dyad through base pair A6·T19 in the Dickerson−Drew dodecamer (Figure 2B; see the duplex at the top) will place the rotated adenine on top of the thymine base, and similarly, the rotated thymine will be placed on top of the adenine base. With this sequence, only two base pairs will be conserved in terms of sequence as a consequence of a rotation around the 2-fold, and for another two, G will be superimposed on A and C will be superimposed on T (Figure 2B).

The two solutions had initially been refined individually in space group *R*3. Subsequently, they were combined by fixing the occupancies of all DNA atoms at 0.5. Further refinement was carried out against expanded *R*32 data, using NCS-restraints to maintain the symmetry between the two three-duplex stacks around the crystallographic dyad. Water molecules and further ions besides the already included chloride anions were assigned to regions of superimposed sum and difference density. The refinement results are summarized in Table 2, and examples of a final omit-type ($2F_o - F_c$) electron density map around various duplex regions are depicted in Figure 3. In general, the *x* and *y* coordinates of a stack running along the *z*-direction of a unit cell can be determined in a straightforward manner. However, determining the correct translational component of individual duplexes along the stacking direction or, in other words, finding the right register, is more problematic. To facilitate the structure determination and to check correctness of the solution, three brominated dodecamers were synthesized (^{Br}C1, ^{Br}C9, and ^{Br}U8), but none of them produced crystals under either the native conditions or slight variations thereof. However, close examination of the arrangement of individual duplexes in the stacks spanning the long dimension of unit cells shows that these columns of duplexes are only pseudocontinuous. The stacks are broken down into units of three duplexes, and these individual stacks feature considerably reduced slides relative to each other compared with intrastack slides (Figure 4 and Table 4; see the Results). By comparison, sliding between duplexes within the stacks is only minimal, giving them the appearance of continuous 36-mer duplexes (Figure 2A). Together with the relatively low final values for both *R* and R_{free} (Table 2) and the well-defined electron density around the final model (Figure 3), this particular stacking geometry provides evidence for the correctness of our structure.

(30) Yeates, T. O. Detecting and Overcoming Crystal Twinning. In *Macromolecular Crystallography*; Carter, C. W., Jr., Sweet, R. M., Eds.; Academic Press: Inc., New York, 1997; Methods in Enzymology Part A, Vol. 276, pp 344−358.

(31) Kim, S.-H. *Science* **1992**, *255*, 1217−1218.

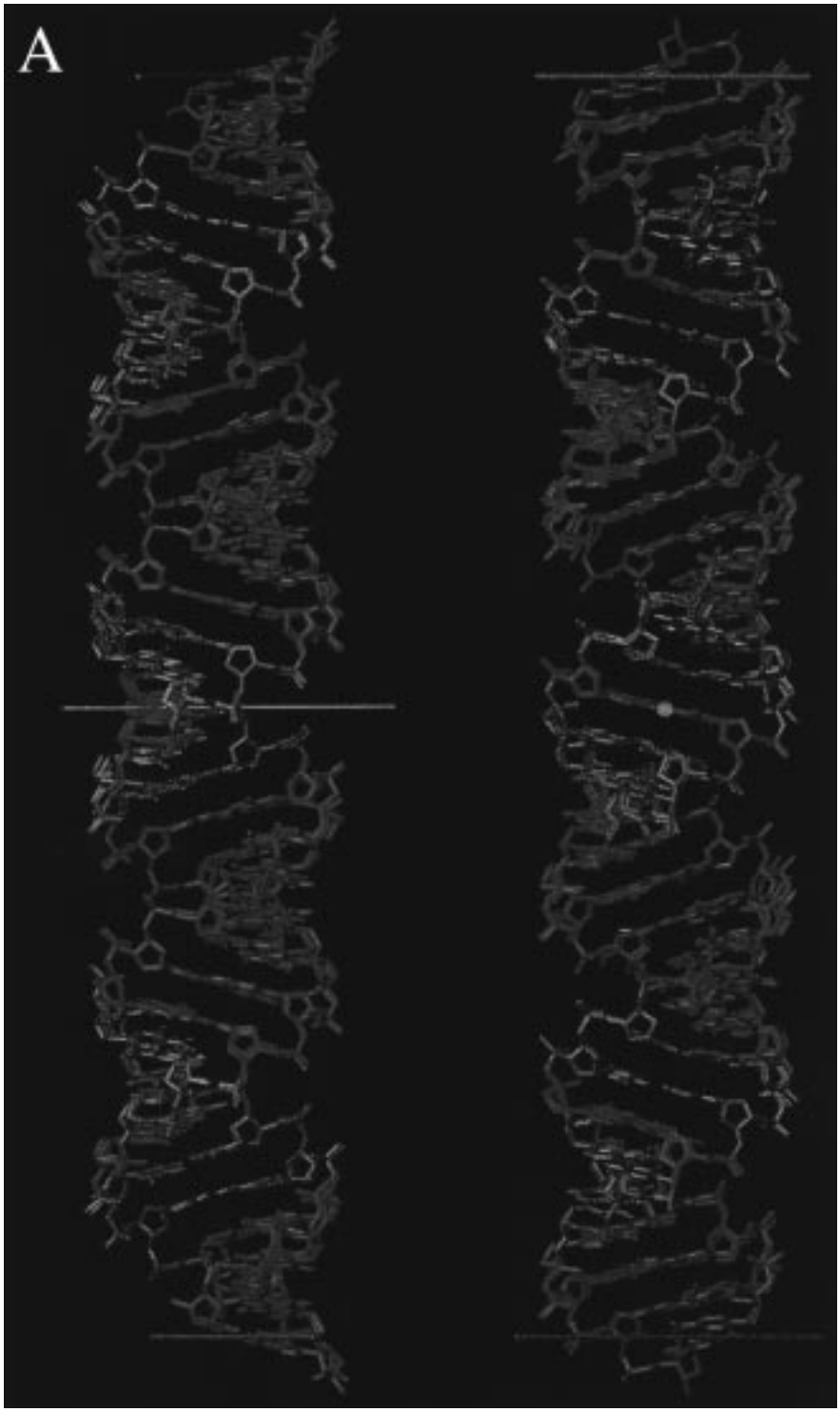

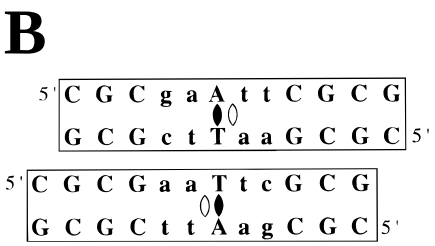

Figure 2. (A) Two views of the two three-duplex stacks, colored in yellow and red, respectively, building up the *R*32 crystal lattice. Duplex 1 is in the center, duplex 2 is at the top, and duplex 3 is at the bottom. View normal to the crystallographic intramolecular dyad which runs through base pair A6·T19 of the middle duplex (left), and rotated around the vertical by 90°, viewed along the intramolecular dyad and into the minor groove of the middle duplex (right). Regions of duplexes for which superimposed purine and pyrimidine bases result as a consequence of a rotation around the central dyad are gray. Intramolecular dyad (center) and intermolecular dyads (top and bottom) are drawn as gray lines. The particular orientation of the three-duplex stack relative to the crystallographic dyad produces overhanging terminal base pairs, visible at the top and at the bottom. Termini from three-duplex stacks located above and below the depicted one are then superimposed on these overhanging base pairs (not shown). (B) Schematic demonstrating the superpositioning of phosphoramidate dodecamer duplexes in the rhombohedral lattice. Rotation around the molecular dyad (open symbol) would reproduce the dodecamer duplex, while rotation around the crystallographic dyad through the sixth base pair (top duplex, filled symbol between A and T) produces a duplex (below) which is slid relative to the original one by one base pair. Small font designates base pairs which are either conserved or have purine overlaid on purine and pyrimidine overlaid on pyrimidine after a rotation around the crystallographic dyad.

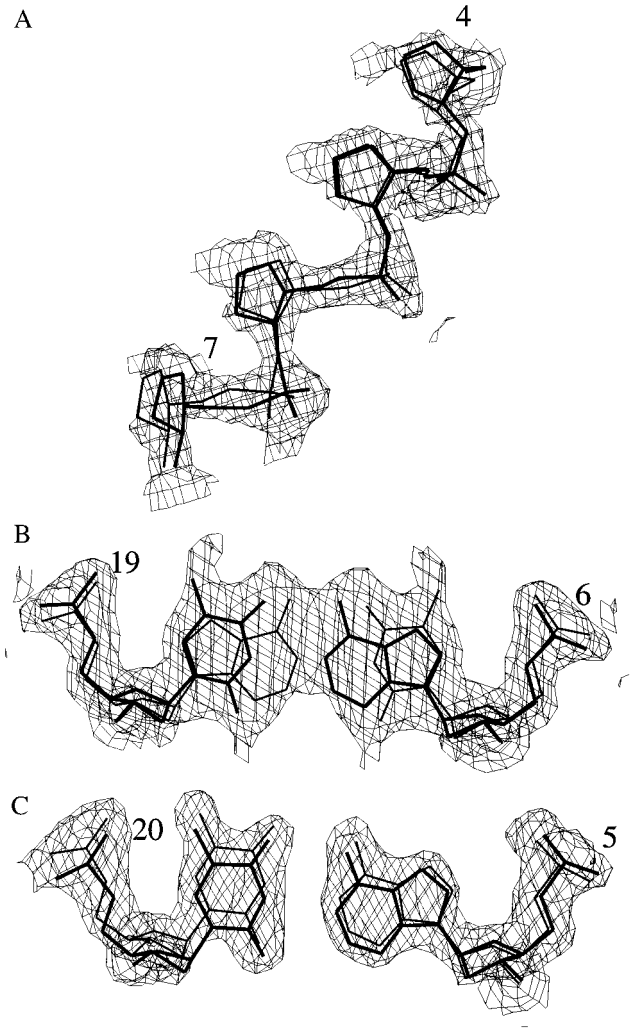

Figure 3. ($2F_o - F_c$) electron density map contoured at a 1σ level around three regions of the three-duplex stack forming the asymmetric unit (see Figure 2 for orientation; # designates symmetry-related residues). The map was generated by omitting from the three duplexes the nucleobases of all residues depicted in capital font in Figure 2B. Thus, we only included backbone atoms and atoms of regions where the positions of purines and pyrimidines are conserved after rotating around the crystallographic dyad. When judging the quality of the map, one should keep in mind that, rather than simply omitting the portion of the molecule around which the map is being displayed (as in a standard omit map), we have actually omitted 30% of the total scattering power per asymmetric unit. (A) Backbone portions of duplexes 1 between nucleotides G4 and T7 and A17# and T20#, respectively; note the near superposition of the two sugar−phosphate backbones despite the location of the crystallographic dyad within base pair A6·T19, rather than between the two central base pairs. (B) Base pairs A6·T19 (bold) and T19#·A6#; the crystallographic dyad runs along the vertical between pairs of overlaid A's and Ts'. (C) Base pair A5·T20 (bold) superimposed on base pair A18#·T7#.

Results

Overall Geometry of the 3′-NP DNA Duplexes. The investigated phosphoramidate DNA crystals contain three crystallographically distinct dodecamer duplexes which display very similar global and local conformations. Despite their similar features, we will provide the geometrical parameters for each of them individually, rather than looking at an averaged structure. Nucleotides of duplex 1 (the one featuring the intramolecular dyad) are numbered 1−24, nucleotides of duplex 2 are numbered 100−124, and nucleotides of duplex 3 are numbered 200−224. Selected overall and local helical parameters for the three duplexes are listed in Table 3. The combined figures are consistent with the conformational characteristics of the A-form duplex family (Table 3). With average helical rise values of around 2.8 Å, the duplexes have somewhat closer resemblance to A-DNA than A-RNA, although the variations in rise between individual crystal structures of DNA and RNA duplexes render a distinction between an A-DNA and an A-RNA family somewhat meaningless. As apparent from Table 3, duplexes 2 and 3 which assume general orientations in the crystal lattice resemble each other more closely and have slightly higher rise and twist values than duplex 1 which lies between them and contains the crystallographic 2-fold rotation axis. The rms deviation between duplexes 1 and 2 is 0.57 Å, between duplexes 1 and 3, it is 0.62 Å, and between duplexes 2 and 3, it is 0.68 Å. The rms deviations for duplexes 1−3 relative to the search model are 0.85, 0.92, and 0.89 Å, respectively. The geometric differences are likely related to the particular position of a duplex in the lattice and may represent the strong pseudosymmetry between the two duplexes in general orientations, due to their arrangements relative to the crystallographic dyad.

Table 3. Selected Global and Local Helical Parameters of the 3′-NP DNA Duplexes[a]

Global Helical Parameters (displacement, width, and depth in angstroms, twist in degrees, and standard deviations in parentheses)

duplex	helix rotation	residues per turn	displacement	major groove width/depth[b]		minor groove width/depth[b]	
1	31.9(2.7)	11.3	2.79(0.14)				
2	32.5(2.8)	11.1	2.84(0.23)	5.3	9.4	10.1	0.3
3	32.7(2.0)	11.0	2.85(0.17)				
A-DNA[c]	32.7(2.0)	11.0	2.73(0.15)	4.2	9.4	10.7	0.2
A-RNA[d]	33.2(1.6)	11.1	2.49(0.13)	6.9	10.0	9.8	0.3
B-DNA[e]	35.5(7.8)	10.1	3.30(0.48)	11.8	4.7	4.8	5.3

Average Local Helical Parameters (rise, slide, *x*-displacement, and *y*-displacement in angstroms, twist, roll, inclination, and propeller twist in degrees, and standard deviations in parentheses)

		base step parameters		
duplex	rise	slide	twist	roll
1	2.78(0.13)	−1.56(0.30)	32.9(2.5)	8.3(3.8)
2	2.84(0.18)	−1.47(0.29)	33.1(2.6)	8.5(3.9)
3	2.86(0.14)	−1.39(0.20)	33.5(2.8)	9.1(3.7)

		base pair parameters		
duplex	*x*-displacement	*y*-displacement	inclination	propeller twist
1	−4.46(0.52)	0.15(0.54)	14.8(1.0)	−10.8(4.0)
2	−4.16(0.34)	0.03(0.34)	14.5(2.3)	−12.8(4.8)
3	−4.04(0.46)	0.34(0.36)	14.8(1.4)	−9.6(2.4)

[a] Calculated with the program NEWHEL93 distributed by R. E. Dickerson. [b] Calculated with the program CURVES.[32] The values refer to the three-duplex stack (3′-NP DNA), a 20-mer duplex based on the central tetramer of $[d(GTGTCACA)]_2$ (A-DNA), a two-duplex stack based on the rhombohedral crystal form of $[r(C_4G_4)]_2$ (A-RNA), and a single $[d(CGCGAATTCGCG)]_2$ duplex (B-DNA). [c] Based on the crystal structure of the A-DNA duplex with sequence 5′-(GTGTACAC) (NDB[33] Code ADH038, resolution 1.40 Å).[34] [d] Based on the rhombohedral crystal form of the A-RNA duplex with sequence 5′-(C_4G_4) (NDB Code ARH074, resolution 1.46 Å).[35] [e] Based on the crystal structure of the Dickerson−Drew B-DNA with sequence 5′-(CGCGAATTCGCG) (NDB Code BDL084, resolution 1.40 Å).[36]

The Phosphoramidate DNA Backbone Conformation. Analysis of the sugar−phosphate backbone torsion angles in the three duplexes reveals unusually small variations among the individual angles throughout the entire 72 nucleotides represented by the three-duplex stack. The average values for backbone torsion angles are (in degrees, standard deviations in

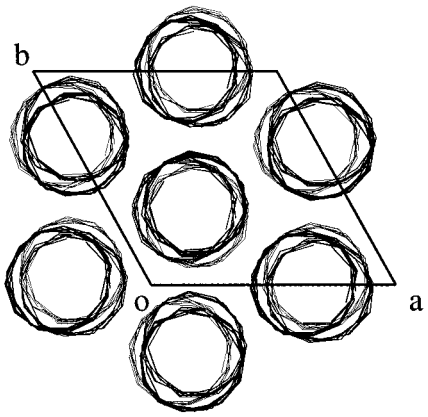

Figure 4. Projection of a unit cell in the 3′-NP DNA dodecamer crystal along the crystallographic *z*-direction. The thickness of the depicted layer corresponds to ca. 304 Å or one *c*-cell constant. This view demonstrates the formation of nearly continuous helixes by three adjacent duplexes (each constituting an asymmetric unit) and the shifting between the three-duplex stacks. Units of three-duplex stacks are schematically represented by vectors connecting their sugar C1′ atoms, the vectors for each stack drawn with lines of different thicknesses (top stack bold, middle stack medium, and bottom stack thin).

parentheses) $\alpha = 294.1(10.7)$, $\beta = 172.7(10.7)$, $\gamma = 54.4(6.3)$, $\delta = 79.3(3.8)$, $\epsilon = 206.6(7.8)$, and $\zeta = 287.4(8.0)$. Without a single exception, the conformations of the torsion angles fall into the ranges (for α to ζ) *−sc*, *ap*, *+sc*, *+sc*, *ap*, and *−sc*, indicative of the A-form backbone. Similarly, all glycosidic conformations are anti (average χ angle 199.4°, standard deviation 5.5°). With very few exceptions, the sugar pucker type is C3′-endo (average pseudorotation phase angle $P = 13.8°$, standard deviation 3.8°). These exceptions are nucleotides 15, 101, 114, 201, 213, and 216, all adopting C2′-exo-type puckers, this range being a direct neighbor of the C3′-endo mode in the furanose pseudorotation phase cycle. The observed degree of conservation for conformational ranges with the 3′-NP DNA dodecamer backbones distinguishes this analogue from both DNA and RNA and strongly suggests that the phosphoramidate DNA duplex is conformationally more rigid compared to the two natural nucleic acid types.

Crystal Packing and Ion Coordination. Interactions between duplexes in the rhombohedral lattice of the 3′-NP DNA crystal occur almost exclusively through stacking between terminal base pairs of adjacent duplexes. In particular, there are no direct lateral contacts between DNA atoms from adjacent duplexes across stacks. All stacking interactions are of the 5′−3′/3′−5′ type, and the infinite stacks running along the crystallographic *z*-direction thus take on the appearance of almost continuous helixes. However, the individual three-duplex units constituting the asymmetric unit are recognizable as such through the distinct degrees of sliding and twisting between them (Figure 4). These relative translations and rotations, respectively, differ from those between duplexes within stacks, the latter ones resembling those in a regular A-type duplex more closely. The helical parameters describing the relative orientations of duplexes within and between three-duplex stacks are listed in Table 4. Compared with slide and twist which differ considerably, the remaining helical parameters, e.g., rise and inclination, are quite similar for intra- and interstack transitions.

Chloride anions occupy a total of 12 sites in the asymmmetric unit of the 3′-NP DNA dodecamer crystal. The ions are located on 3-fold rotation axes running parallel to the crystallographic *z*-direction and therefore parallel to the overall helix axis of duplex stacks. Thus, each site is shared among three adjacent

Table 4. Selected Helical Parameters for Duplex Stacking within (2−1 and 1−3) and between ($3^{\#}$−2) Three-Duplex Stacks[a] (rise and slide in angstroms, twist and roll in degrees)

		base step parameters		
transition	rise	slide[b]	twist[b]	roll
$3^{\#}$−2[c]	2.65	**−0.68**	**43.8**	4.5
2−1	2.53	−1.40	30.1	8.2
1−3	2.69	−1.54	32.8	6.5

[a] Choosing the crystallographic *z*-direction as the overall helical axis. [b] The distinct degrees of sliding and twisting for the transition between three-duplex stacks relative to those between duplexes within stacks are highlighted in bold font. [c] # denotes a symmetry-related duplex, the symmetry operator being a 3-fold screw axis.

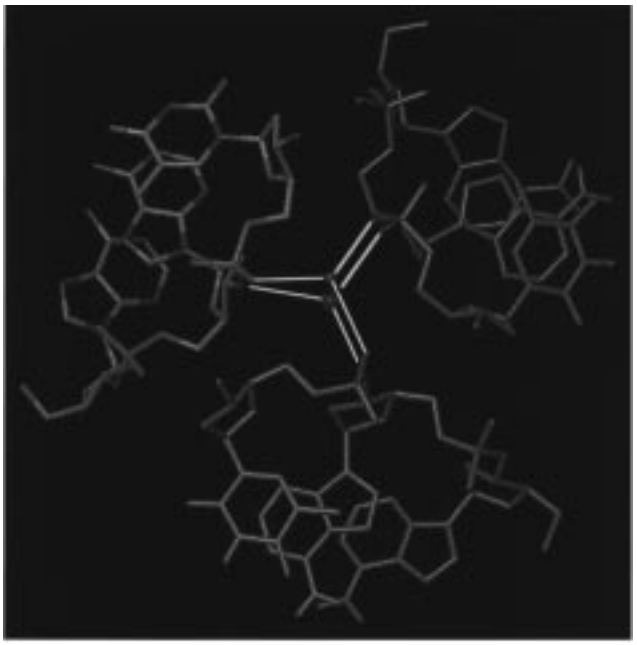

Figure 5. Example of the interaction between phosphoramidate moieties and ammonium and chloride ions in the crystal lattice of the 3′-NP DNA dodecamer. The view is roughly along the 3-fold rotation axis, depicting an ammonium ion (cyan) and a chloride ion (green) forming hydrogen bonds to three phosphate oxygens and amidate nitrogens, respectively. A similar ion coordination mode is found at 11 additional sites in the asymmetric unit. Atoms of the original duplex are colored individually, yellow for carbon, red for oxygen, cyan for nitrogen, and orange for phosphorus. Atoms of the two adjacent symmetry-related duplexes are colored pink and green, respectively, and hydrogen bonds are thin white lines (for distances see the text).

asymmetric units, and taking into consideration the occupancy of one-third for each of the chlorides, there are then four of them per asymmetric unit. Each of the three phosphoramidate duplexes per asymmetric unit forms four direct contacts to chloride anions. The chlorides are sitting in the channels that are formed between three infinite stacks and are engaged in three hydrogen bonds to 3′-amino groups of backbones (Figure 5; the N(H)···Cl^- distances lie between 3.21 and 3.35 Å for the various interactions). Each of the chloride ions is engaged in a fourth hydrogen bond to an ammonium ion, also positioned on the 3-fold rotation axis (Figure 6; the Cl^-···$N(H)_4^+$ distances lie between 2.44 and 3.32 Å for the various interactions). An additional ammonium ion, also situated on the 3-fold, is found in the vicinity of each of the chlorides (distances between 3.77 and 4.45 Å). These ammonium ions form hydrogen bonds to phosphate oxygens from three symmetry-related duplexes (Figure 5; the $N(H)_4^+$···($^-$O)P distances lie between 2.35 and

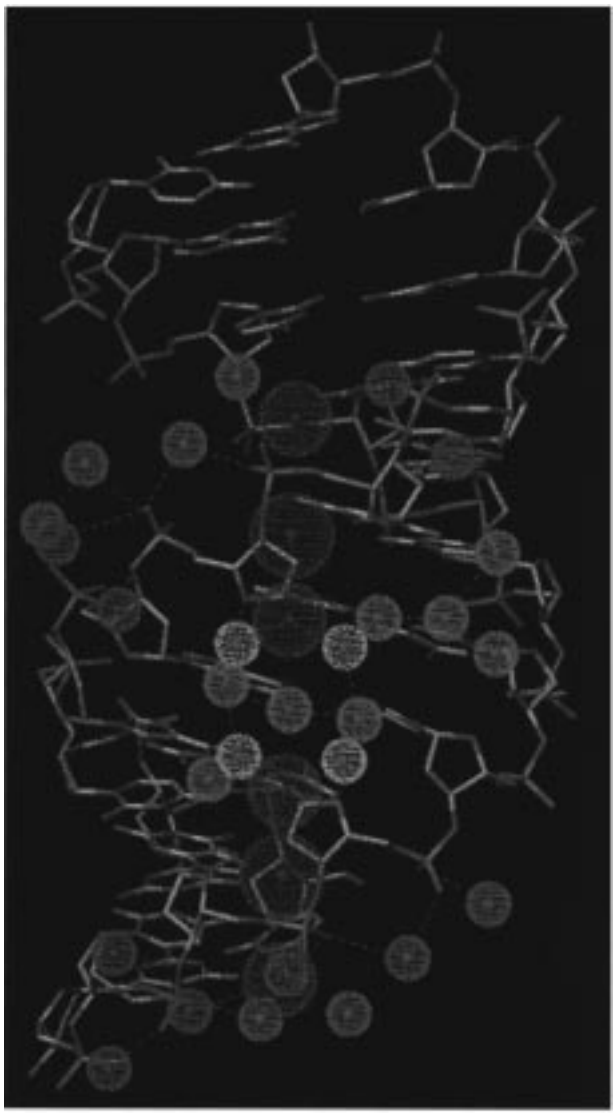

Figure 6. Formation of a water bridge across the minor groove of duplex 1, featuring the intramolecular dyad. Water molecules and ions are represented as balls as well as larger dotted surface spheres, colored according to their location on the duplex surface. Water molecules are pink balls; dotted spheres around waters bound to phosphate oxygens are red, those bound to or stabilized by the 3′-amidate nitrogens are cyan, those bound to base atoms or with no direct DNA contacts are orange, and spheres around waters coordinated to ammonium ions are yellow. Chloride ions are green balls, and cyan spheres around them are drawn with a larger radius. Ammonium ions are blue balls, their cyan spheres drawn with a medium radius. Hydrogen bonds are dashed magenta lines. The chloride in the center of the drawing and the one closer to the duplex terminus below it are bound to opposite strands and act as bridge heads for the chain of ammonium ions and water molecules running across the groove. The bridge runs approximately parallel to the helical axis, the crossing distance being somewhat longer than the narrowest dimension of the minor groove. The approximate local 2-fold symmetry of the hydration pattern is apparent (the local dyad runs roughly vertical to the paper plane and through the orange water surrounded by four yellow waters). This local dyad is different from the crystallographic dyad running through the sixth base pair of this duplex. A similar hydration pattern is also present in the minor groove of the upper half of the duplex (not shown). Overall, this type of hydration bridge is observed six times in the three duplexes constituting the asymmetric unit.

3.22 Å for the various interactions). There are thus a total of 24 ammonium ion sites per asymmetric unit, each of them with occupancy one-third.

The formation of direct hydrogen bonds between chloride anions and backbone 3′-nitrogens provides a very simple means to determine the configuration of the 3′-nitrogens or, in other words, to distinguish between the orientations of the hydrogen atom and the lone electron pair on the sp^3-hybridized 3′-nitrogens (Figure 5). Thus, assuming a more or less linear hydrogen bond between the amino group and chloride ion (consistent with a stretched N−H···Cl^- angle), the lone electron pair is located between the nonbridging oxygen atoms of the 5′-phosphate group. This is in full agreement with a strong anomeric effect between the lone electron pair and antibonding σ^* orbital of the P−O5′ bond (see the Discussion).

The chloride anions form a superlattice which is itself compatible with the symmetry of space group *R*32. Pairs of chloride anions serve as bridge heads for water bridges across the minor groove (Figure 6). The chlorides bind to amino nitrogens from opposite strands, the nitrogens spaced by three base pair steps (Figure 6). Thus, there are totally six of these chloride tandems, bracing the minor grooves of the three phosphoramidate duplexes. The strongly conserved coordination pattern between chlorides and 3′-amino nitrogens of phosphoramidate backbones is very suggestive of a crucial role of the anions in the formation of the 3′-NP DNA lattice. One is led to speculate that the chlorides, to optimize their coordination geometry as well as to satisfy their spatial requirements, force the phosphoramidate duplexes into an arrangement that is only halfway compatible with the intrinsic symmetry of the duplexes. Whereas the symmetry of space group *R*32 fits the organization of the chlorides and their associated ammonium ions, the duplexes cannot align their molecular dyads with the crystallographic ones, hence the unusual composition of crystals with two duplex stacks, their relative rotations and translations in terms of the dyad being ±16° and one-half of a base step up or down, respectively. As noted earlier, the important role of chloride and ammonium ions for lattice formation is in agreement with the fact that 3′-NP DNA dodecamer crystals suitable for diffraction experiments could not be obtained without the use of this particular salt.

Amidate Backbone and Groove Hydration. The particular positioning of duplexes relative to the crystallographic dyads in the 3′-NP DNA crystal results in two superimposed stacks (Figure 2). This means that each base pair of one duplex is only half-occupied, with the other half contibuted by a base pair of a duplex from the symmetry-related stack. In most cases, the base composition of a particular pair is not retained; rather a purine base is placed over a pyrimidine base and vice versa (Figure 2B). However, as pointed out earlier, the backbones of duplexes from symmetry-related stacks are nearly superimposed (Figures 2A, 3A). A water molecule which is hydrogen bonded to a backbone 3′-nitrogen of one duplex will therefore also be engaged in a hydrogen bond to the amino nitrogen of the overlaid duplex from the symmetry-related stack, and the hydrogen bond distances will deviate only slightly. In electron density maps, such water molecules usually appeared as a single peak and their positions were refined with full occupancies. It is clear that statements based on our structure concerning the hydration of bases are somewhat limited. For example, in a case where a thymine and an adenine are placed on top of each other, a water molecule in the minor groove might be hydrogen bonding to the O2 of thymine (with a 50% occupancy of that position), or to the N3 of adenine (also 50%). Alternatively, both bases in the individual superimposed duplexes could be hydrated at that site, and the water molecule would then have to be treated with a 100% occupancy, although the distances to

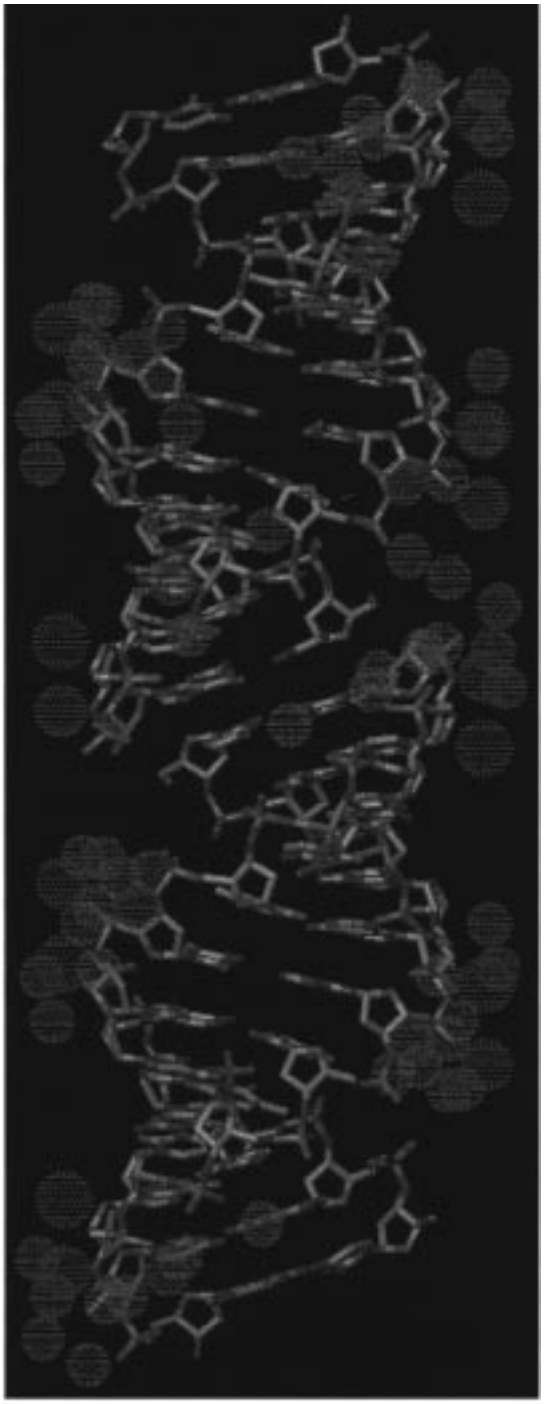

Figure 7. Overall view of the backbone hydration for dodecamer duplexes 1 (bottom) and 2. Water molecules are depicted as spheres with dotted surfaces and display a contact to a backbone atom with a distance of 3.5 Å or less. Cyan spheres are water molecules which either form a direct hydrogen bond to a 3′-amino nitrogen or are part of the water bridges (ususally two water molecules) that link nonbridging phosphate oxygens and 3′-nitrogens. Thus, the presence of all water molecules in cyan can be attributed to the 3′-amino group in the backbone of 3′-NP DNA. Red water molecules are hydrogen bonded to phosphate oxygens and could in principle also be bound to the native DNA phosphodiester backbone. This includes water molecules that are arranged between nonbridging phosphate oxygens from adjacent intrastrand residues in either A-DNA or A-RNA. DNA carbons are yellow, oxygens are red, nitrogens are cyan, and phosphorus atoms are orange.

the two base acceptors would obviously be different. A total of 34 water molecules with full occupancy and direct hydrogen

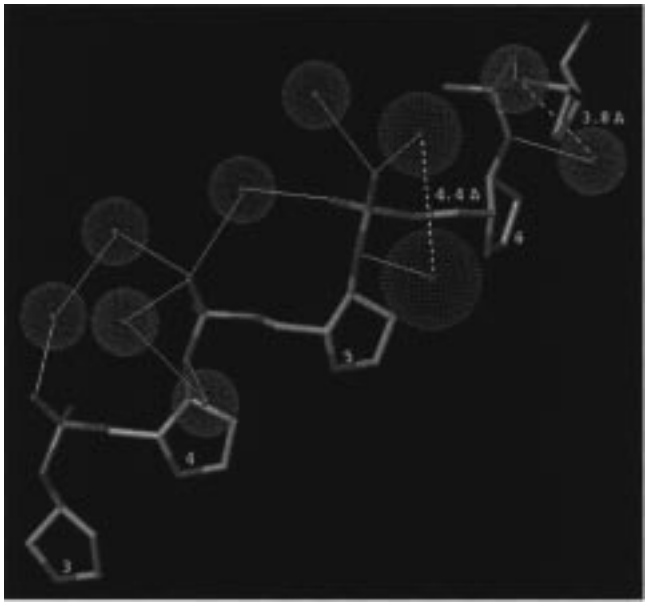

Figure 8. Hydration of the 3′-NP DNA backbone. A recurring pattern is depicted, with each phosphoramidate moiety surrounded by four water molecules. Two water molecules (cyan spheres) link the 3′-amino nitrogen to a nonbridging phosphate oxygen. In some cases, these water molecules are replaced by an ammonium ion (upper green sphere, hydrogen bonded to the phosphate oxygen) and a chloride ion (lower green sphere, hydrogen bonded to the 3′-nitrogen). Red spheres represent water molecules which are hydrogen bonded to phosphate oxygens and could thus be present in DNA as well. A fifth water molecule per phosphoramidate moiety is usually bound to the second nonbridging phosphate oxygen, pointing away from the reader (not shown). Nucleotides are numbered, 3′-NP DNA carbons are yellow, oxygens are red, nitrogens are cyan, and phosphorus atoms are orange. Hydrogen bonds are thin white lines, and only distances longer than 3.5 Å are included. The color scheme and orientations are consistent with those of Figure 6.

bonding contacts to bases were placed in the minor and major grooves of the superimposed 1.5 duplexes, forming the asymmetric unit in space group *R*32. However, since the chemical modification in 3′-NP DNA concerns the backbone, it will be most interesting to determine the changes in the hydration of the backbone. One might expect only subtle alterations in the previously observed base hydration patterns of DNA as a consequence of replacing O3′ by an amino group.

The analysis of the arrangement of water molecules around the phosphoramidate backbone reveals that the 3′-amino groups are well hydrated, with many of them forming hydrogen bonds to one or even two water molecules. Figure 7 shows the distribution of water molecules around the backbones of the stacked duplexes 1 and 2. It is noteworthy not only that the presence of a donor function adjacent to the phosphate group results in a higher number of water molecules directly bound to that donor but, in addition, that many water molecules are immobilized on the backbone by interacting with the former ones, often linking the nitrogen-bound waters to negatively charged phosphate oxygens. A hydration pattern that was observed with quite a few phosphoramidate moieties comprises four to five water molecules (Figure 8). Two water molecules link the 3′-nitrogen to a nonbridging phosphate oxygen, and the phosphate oxygen itself shares two water molecules with phosphate oxygens from 5′- and 3′-adjacent nucleotides. A further water molecule is hydrogen bonded to the second nonbridging phosphate oxygen. Alternatively, two water molecules are hydrogen bonded to the 3′-nitrogen, and the distances between either of them and the water molecule bound to the

phosphate oxygen are then slighly too long to be considered relevant hydrogen bonds (not shown). The first pattern remains intact when the two water molecules bridging nitrogen and phosphate oxygen are replaced by an ammonium and a chloride ion, respectively (Figure 8). The chloride ion is hydrogen bonded to the 3′-nitrogen, and the ammonium ion takes the place of the water bound to the phosphate oxygen. The distance between the chloride and this ammonium ion is longer than 4 Å (Figures 5 and 8), and the chloride ion is engaged in a direct hydrogen bond to a second ammonium ion located in the minor groove (Figure 6). The latter interaction is part of a bridge consisting of ions and water molecules which spans the entire minor groove across strands (Figure 6). By interacting with the chloride ions on the groove borders, the 3′-nitrogens serve as bridge heads. Thus, the presence of 3′-amino groups in the phosphoramidate backbone not only brings about a superb hydration of the sugar−phosphate portion of the duplex but stabilizes the groove hydration as well. The minor groove spanning bridge is present at five other sites in the three phosphoramidate duplexes. The individual trinucleotide duplexes which are spanned by the bridges feature different sequences, and the water bridge formation therefore appears to be sequence-independent.

Discussion

Structural and Stereoelectronic Consequences of Replacing O3′ by an Amino Group. In nucleosides, nucleotides and oligonucleotides, the pseudorotational equilibrium between the two fundamental conformational states of the furanose moiety, N or C3′-endo/C2′-exo and S or C2′-endo/C3′-exo, respectively, is influenced by a variety of steric and stereoelectronic effects within the sugar portion (gauche effect) and between sugar and nucleobase (anomeric effect).[37] In DNA, there are two basic stereoelectronic effects which oppose each other. One is the gauche effect [*O4′*−C4′−C3′−*O3′*−PO_3H^-] between O3′ and O4′, which has been shown to drive the conformational equilibrium toward S. The other is the anomeric effect which drives the sugar conformational equilibrium toward N, to position the base heterocycle in a pseudoaxial manner for maximal interaction between the C1′−N glycosidic bond and the O4′ α-lone pair. Replacing the 3′-oxygen by an atom or a functional group with decreased electronegativity, for example, by an amino group as in 3′-NP DNA, can be expected to significantly alter the gauche effect between the 3′-substituent and the furanose 4′-oxygen. In essence, the gauche effect would become weaker and the opposing anomeric effect should take over as the main force dictating the conformational equilibrium. Indeed, our structure of the phosphoramidate DNA dodecamer reveals an A-type duplex conformation with 66 of the 72 nucleotides per asymmetric adopting C3′-endo type deoxyribose-sugar puckers. The B-type conformation assumed by the unmodified Dickerson−Drew DNA dodecamer with identical sequence[24] has been firmly established by dozens of X-ray crystal structures over the last 15 years.[36] Moreover, CD-spectra of the 3′-NP DNA dodecamer are consistent with adoption of an A-RNA conformation by the modified oligonucleotide in solution as well.[10] Therefore, we conclude that, as a main consequence, replacement of the DNA 3′-oxygen by an amino group locks the (phosphoramidate) DNA duplex conformation in the A-form.

The conformational uniformity of the backbone in the phosphoramidate DNA duplex is apparent from both conserved sugar puckers and minimal variations in the six backbone torsion angles among individual nucleotides. Almost all of the latter ones display rms deviations in the single digits, a finding that is in stark contrast to the relative flexibility of backbones in nucleic acid double helixes of the A-, B−, and Z-types. All three come in not just one rigid form, but exhibit a range of conformations, depending on sequence,[38] counterions,[39] crystal packing forces,[40] and interactions with drugs[41] and proteins.[42] Conformational polymorphism was observed in the backbones of most right- and left-handed duplexes, and in B-DNA and Z-DNA, these are referred to as B_I and B_{II}[43] as well as Z_I and Z_{II},[44] respectively. Notably, in the backbones of A-type duplexes, both DNA[45] and RNA,[27] a local crankshaft motion around torsion angle β converts the standard (α−*sc*, γ +*sc*) to an extended (α *ap*, γ *ap*) conformation. Conversely, the backbone conformation in the phosphoramidate A-type duplex is uniform, and not a single nucleotide is flipped into the extended form. The recurring coordination of chloride anions and water molecules to 3′-amino groups hints at the origins of the exceptional rigidity of the phosphoramidate backbone. As mentioned earlier, the presence of ions hydrogen bonded to certain backbone amino groups allows a distinction between the nitrogen lone pair and hydrogen. The acceptance of the amino hydrogen by a chloride anion renders the N3′ more negative. The observed antiperiplanar orientation between the nitrogen lone pair and P−O5′ bond will then bring about a stronger conjugation between the nitrogen lone electron pair and the antibonding σ^* orbital of the adjacent P−O5′ bond (Figure 9A). Indeed, this anomeric effect and the one between O5′ and the antibonding σ^* orbital of the adjacent P−O3′ bond were postulated as being responsible for the preferred (−*sc*, −*sc*)

(32) Program CURVES, Version 4.1. (a) Lavery, R; Sklenar, H. *J. Biomol. Struct. Dyn.* **1988**, *6*, 63−91. (b) Lavery, R; Sklenar, H. *J. Biomol. Struct. Dyn.* **1989**, *7*, 655−667.

(33) Berman, H. M.; Olson, W. K.; Beveridge, D. L.; Westbrook, J.; Gelbin, A.; Demeny, T.; Hsieh, S.-H.; Srinivasan, A. R.; Schneider, B. *Biophys. J.* **1992**, *63*, 751−759.

(34) Thota, N.; Li, X. H.; Bingman, C.; Sundaralingam, M. *Acta Crystallogr., D* **1993**, *46*, 282−291.

(35) Egli, M.; Portmann, S.; Usman, N. *Biochemistry* **1996**, *35*, 8489−8494.

(36) Shui, X.; McFail-Isom, L.; Hu, G. G.; Williams, L. D. *Biochemistry*, in press.

(37) (a) Plavec, J.; Weimin, T.; Chattopadhyaya, J. *J. Am. Chem. Soc.* **1993**, *115*, 9734−9746. (b) Plavec, J.; Thibaudeau, C.; Chattopadhyaya, J. *J. Am. Chem. Soc.* **1994**, *116*, 6558−6560. See also cited in both.

(38) (a) Kennard, O.; Hunter, W. N. *Angew. Chem., Int. Ed. Engl.* **1991**, *30*, 1254−1277. (b) Dickerson, R. E. DNA Structure from A to Z. In *DNA Structures*; Lilley, D. M. J., Dahlberg, J. E., Eds.; Academic Press, Inc.: San Diego, CA, 1992; Methods in Enzymology Part A, Vol. 211, pp 67−111. (c) Egli, M. Structural Patterns in Nucleic Acids. In *Structure Correlation*; Bürgi, H.-B., Dunitz, J. D., Eds.; VCH Publishers, Inc.: New York, 1994; Vol. 2, pp 705−749. (d) Grzeskowiak, K. *Chem. Biol.* **1996**, *3*, 785−790. (e) Hartmann, B.; Lavery, R. *Q. Rev. Biophys.* **1996**, *29*, 309−368.

(39) See e.g.: Egli, M.; Williams, L. D.; Gao, Q.; Rich, A. *Biochemistry* **1991**, *30*, 11388−11402.

(40) (a) Shakked, Z.; Guerstein-Guzikevich, G.; Eisenstein, M., Frolow, F.; Rabinovich, D. *Nature* **1989**, *342*, 456−460. (b) Jain, S.; Sundaralingam, M. *J. Biol. Chem.* **1989**, *264*, 12780−12784. (c) Ramakrishnan, B.; Sundaralingam, M. *J. Biomol. Struct. Dyn.* **1993**, *11*, 11−26.

(41) See reviews in ref 38; a recent example is the complex between a DNA duplex and the anticancer drug cisplatin: Takahara, P. M.; Rosenzweig, A. C.; Frederick, C. A.; Lippard, S. J. *Nature* **1995**, *377*, 649−652.

(42) Among the many examples of protein-induced DNA conformational changes, see: Guzikevich-Guerstein, G.; Shakked, Z. *Nature Struct. Biol.* **1996**, *3*, 32−37 and cited therein.

(43) (a) Fratini, A. V.; Kopka, M. L.; Drew, H. R.; Dickerson, R. E. *J. Biol. Chem.* **1982**, *257*, 14686−14705. (b) Cruse, W. B. T.; Salisbury, S. A.; Brown, T.; Cosstick, R.; Eckstein, F.; Kennard, O. *J. Mol. Biol.* **1986**, *192*, 891−905. (c) Privé, G. G.; Yanagi, K.; Dickerson, R. E. *J. Mol. Biol.* **1991**, *217*, 177−199.

(44) Wang, A. H.-J.; Quigley, G. J.; Kolpak, F. J.; van der Marel, G. A.; van Boom, J. H.; Rich, A. *Science* **1981**, *211*, 171−176.

(45) Haran, T. E.; Shakked, Z.; Wang, A. H.-J.; Rich, A. *J. Biomol. Struct. Dyn.* 1987, *5*, 199−217.

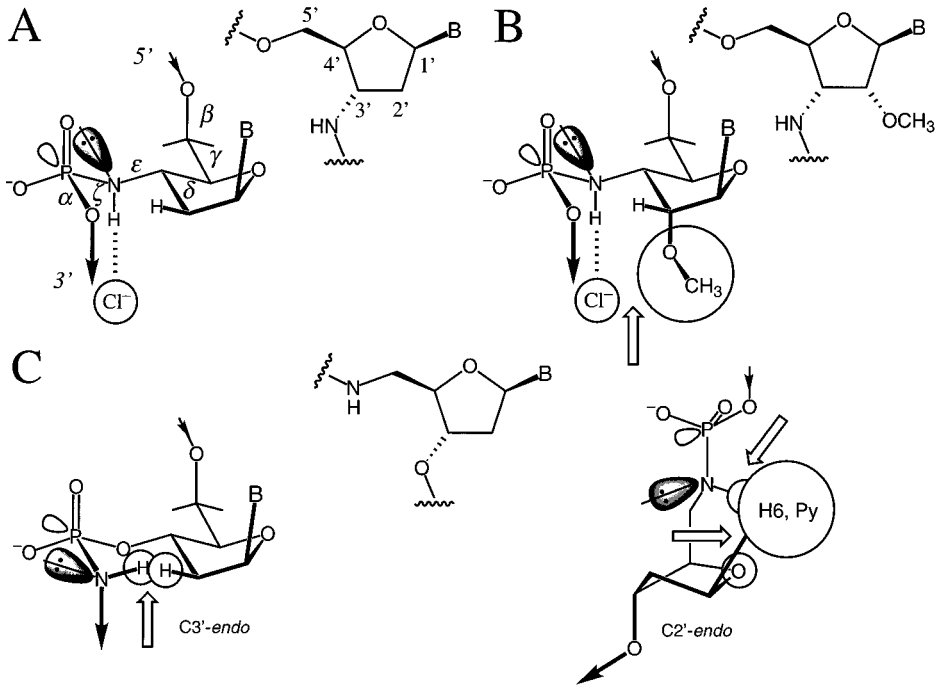

Figure 9. Conjugative and steric effects in phosphoramidate DNA. (A) Anomeric effect between the N3′ lone electron pair and the antibonding σ^* orbital of the P−O5′ bond in N3′ → P5′ phosphoramidate DNA. The hydrogen bond between the amino group and chloride ions or water molecules renders the nitrogen more negative, strengthening the conjugation to the antiboding orbital of the P−O bond and fixing torsion angle ζ in a −*sc* conformation. (B) The presence of a bulky 2′-*O*-substituent will negatively affect hydrogen bond formation through a 1,5-repulsion (open arrow). This may explain why the 2′-*O*-methyl-3′-NP DNA modification leads to reduced RNA affinity compared with phosphoramidate DNA. However, small or polar substitutents, the latter ones capable of sharing a water molecule with the 3′-amino nitrogen, should in principle not disrupt self-pairing. This is consistent with the observed high affinity of 2′-fluoro-3′-NP DNA for RNA. The depicted *ap* orientation of the C2′−C3′ and O2′−CH_3 bonds is in accordance with the conformation of a 2′-methoxy sugar in a recent crystal structure of a modified A-form duplex.[48] (C) Putative conjugation between the N5′ lone pair and the antibonding σ^* orbital of the P−O3′ bond with P → N5′ phosphoramidate DNA. Using the same argument as before, this conjugation would fix torsion angle α in a −*sc* conformation. Provided the furanose adopts an A-type pucker, this arrangement would result in a steric repulsion between the 5′-amino hydrogen and a 2′-hydrogen of the deoxyribose (open arrow, left). Adoption of a standard B-type conformation is prohibited by short contacts that would arise between the 5′-amino hydrogen and O4′ on one hand (ca. 2.3 Å) and H6 of pyrimidine on the other (ca. 2.2 Å, open arrows, right). Neither conformation renders the amino proton accessible for hydrogen bond acceptors. The importance of N3′-hydration for conformational stability in the case of 3′-NP DNA strongly suggests that the inability of 5′-PN DNA to pair with RNA is related to the absence of such hydrogen bonds in its backbone and the concomitant reduction of hydration.

phosphodiester conformation (torsion angles α and ζ) in nucleic acid double helixes.[46] Therefore, it appears that the replacement of O3′ by an amino group results in a stronger anomeric effect that prevents any significant torsional flexibility around angle ζ and also seems to affect rotational freedom about torsion α. At locations where a chloride anion is hydrogen bonded to the amino group, one of the nonbridging oxygens from the adjacent phosphate group is contacting an ammonium ion, consistent with the buildup of more negative charge at this site.

Phosphoramidate DNA shows higher resistance to nucleases than DNA and RNA,[9,10] and the above finding of a strong anomeric effect in the N3′ → P5′ backbone may shed light on the reduced reactivity of the phosphoramidate relative to the phosphodiester group in DNA. DNA as the genetic material should be reasonably stable, and the rate of hydrolysis of its linking groups should be kept at a minimum,[47] hence the negative charge of the phosphate which drastically diminishes the rate of nucleophilic attack on the ester compared with a neutral or positively charged species. Replacing the phosphate ester with a phosphoramidate reinforces this effect through the described conjugation and renders the phosphate group less reactive to nucleophilic attack. Several other surprising and previously unexplained observations with phosphoramidate DNA can be rationalized now that we know its precise three-dimensional structure and ionic environment. For example, combining the N3′ → P5′ backbone modification with a single 2′-methoxy sugar modification apparently destabilizes the DNA:RNA hybrid duplex.[20] However, 2′-methoxy DNA is known to form more stable duplexes with RNA relative to the corresponding DNA:RNA duplexes.[21] Moreover, oligonucleotides which feature a combination of the N3′ → P5′-modified backbone with 2′-deoxy-2′-fluoro-modified sugars pair much more stably with RNA than the corresponding phosphoramidate DNA strands.[19] For an idealized all-staggered backbone conformation based on the observed geometry in the crystal structure, the presence of an an ion or water molecule accepting a hydrogen bond from the 3′-amino group may lead to a 1,5-repulsion with a bulky 2′-substituent such as the methoxy group (Figure 9B). By comparison, a smaller and more polar substituent such as fluorine can be accommodated more easily and may even lead to a favorable interaction if the hydrogen bond acceptor is a water molecule. Even more difficult to understand than the divergent influences on RNA affinity by various 2′-substituents in 2′-modified 3′-NP DNA was the fact that replacement of the 5′-oxygen by an amino group completely abolishes the ability of the resulting oligonucleotide to pair either with itself or with RNA.[10] Similar to the case of 3′-NP DNA, one can invoke an anomeric effect between the N5′ lone pair and the antibonding σ^* orbital of the P−O3′ bond (Figure 9C).

(46) Eschenmoser, A.; Dobler, M. *Helv. Chim. Acta* **1992**, *75*, 218−259.
(47) Westheimer, F. H. *Science* **1987**, *235*, 1173−1178.

Table 5. Comparison of the Thermodynamics of Self-pairing for 3′-NP DNA, DNA, and RNA[10]

sequence	T_m (°C)[a]	ΔG (kcal/mol)[b]	ΔH (kcal/mol)[b]	ΔS (kcal/mol)[b]
DNA d(CGCGAATTCGCG)	58.0	−12.8	−59.6	−0.151
3′-NP DNA d(CnpGnpCnpGnp-AnpAnpTnpTnpCnpGnpCnpG)	84.0	−17.0	−94.8	−0.251
RNA r(CGCGAAUUCGCG)	66.4	−14.5	−67.0	−0.169

[a] In 10 mM Tris·HCl, pH 7.0, 150 mM NaCl. [b] At 37 °C.

Again, the nitrogen lone pair would be placed between the two nonbridging phosphate oxygens, similar to the situation in 3′-NP DNA. However, rather than being in an axial position, directed away from the sugar and accessible to solvent as in 3′-NP DNA, the amino hydrogen would now clash with one of the sugar 2′-hydrogen atoms. The steric conflict resulting from a replacement of O5′ by an amino group is worsened by the fact that the amino hydrogen is completely inaccessible to a potential acceptor, be it an ion or a water molecule, as this location is now occupied by the sugar with either an N- or an S-type pucker.

Correlating Structure and Stability. Hydration. Our crystal structure has revealed a considerably improved hydration of the 3′-NP DNA backbone relative to DNA as a result of the presence of the amino group. In DNA, the hydrogen bond donors are all located at the floor of the grooves, whereas the backbones feature only acceptor sites. Among the hydrogen bond acceptors, the anionic nonbridging phosphate oxygens are hydrated the best and the chain oxygens O5′ and O3′ are hydrated the least, with the hydration of the furanose 4′-oxygens being intermediate.[49] The donor qualities of the 3′-amino groups in phosphoramidate DNA are far superior to the acceptor qualities of the DNA 3′-oxygens, on the basis of the hydration of the latter in crystal structures. It has been shown that the ribose 2′-hydroxyl group in RNA leads to a dramatically improved hydration of both backbone and grooves.[8,35] The 2′-hydroxyl groups are surrounded by up to three water molecules and can thus function as mediators between phosphate and base hydration. Like the 2′-hydroxyls in RNA, the 3′-amino groups in phosphoramidate DNA represent the only donor moieties in an otherwise donor-deprived region of the duplex. Although the amino groups are situated in the backbone rather than at the periphery of the groove, we find that at several sites, similar to the situation in RNA, the amino groups serve as bridge heads and stabilize a string of water molecules that runs across the minor groove.

In the case of RNA, the improved hydration goes along with an enthalpy-driven higher overall stability of duplex formation relative to DNA, whereas DNA duplex formation is favored entropically.[35] The thermodynamic parameters for duplex formation with 3′-NP DNA, DNA, and RNA based on concentration-dependent UV-melting profiles are listed in Table 5. Accordingly, the T_m of the 3′-NP DNA dodecamer with the Dickerson−Drew sequence lies ca. 18 and 25 °C above those of the RNA and DNA dodecamers, respectively, all featuring the CGCGAATTCGCG sequence (U instead of T in the case of RNA). Interestingly, the stability gain appears to be mostly enthalpy-driven, while the loss of entropy upon formation of the duplex is even more severe for 3′-NP DNA than for RNA (Table 5). However, 3′-NP DNA duplex formation is strongly favored enthalpically over RNA duplex formation. Although there is clear evidence from the crystal structure that the hydration of phosphoramidate DNA is dramatically improved compared to DNA, there is no indication that the 3′-amino groups are more extensively hydrated than the 2′-hydroxyl groups in RNA.

What then could be the cause of the additional improvements in the enthalpy term with 3′-NP DNA duplex formation relative to RNA? The observation that anions form close contacts to the double helix, the chlorides are actually located around 4 Å from the negatively charged phosphates on average, appears to be a unique feature of the phosphoramidate DNA crystal structure. Cations, such as sodium ions or magnesium ions, and other divalent metal ions as well as organic polycations (e.g., spermine) are much more commonly encountered in the crystal lattices of nucleic acid duplexes. We can only speculate that anions are also arranged around the 3′-NP DNA backbones in solution. Immobilizing cations as well as anions on the surface of the double helix in addition to water molecules would certainly contribute positively to the gain in hydrogen bonding enthalpy. However, it is obvious that the anion coordination is indicative of an altered polarity of the backbone and bordering groove regions in phosphoramidate DNA compared with DNA and RNA (Figure 10). As can be seen from the illustrations in Figure 10, the reduced negative potential in the case of 3′-NP DNA is particularly obvious in the vicinity of the phosphate oxygens which rim the shallow groove. In fact, the shallow groove of the 3′-NP DNA duplex appears to be overall slightly less negatively polarized than in DNA and RNA.

A further contribution to the enthalpic stabilization of 3′-NP DNA duplex formation could stem from the strong anomeric effect that exists between the nitrogen lone pair and the adjacent *ap*-oriented P−O5′ bond. It is difficult to quantifiy this contribution, but its importance is evident from the conformational rigidity of the phosphoramidate backbone in the crystal structure and the strict −*sc*, −*sc* conformation of the phosphoramidate moieties. The latter feature is in contrast to the relative flexibility of the A-DNA and A-RNA backbones with frequent occurrences of a so-called extended backbone geometry, where torsion angles α and γ flip into an *ap* conformation. Relative to the situation in standard DNA, this anomeric effect is likely to further reduce the gauche effect between the 3′-substituent and furanose O4′ (and thus the tendency for an S-type pucker), the substitution of oxygen by nitrogen already leading to an increased trend for adoption of an N-type pucker.[50] This is consistent with the observation based on solution NMR experiments that the percentage of N sugar puckering is higher in the 3′-NP DNA duplex than in the TnpT dimer.[12] While this effect can partly account for the significant enthalpic stabilization of duplex formation with 3′-NP DNA, it will also lead to a more unfavorable entropic term. This is precisely what is observed in the concentration-dependent UV-melting experiments (Table 5).

The backbone conformation adopted by the 3′-NP DNA duplex in the crystal permits an extensive hydration of the 3′-amino group, as both the lone electron pair and hydrogen are directed to the outside and therefore freely accessible on the surface. Quite a different situation would be encountered in the case of a backbone with O5′ replaced by an amino group (5′-PN DNA, Figure 9A,C). Not only would there be a steric conflict between the amino hydrogen and H2′^{Si} from the sugar, but the amino group would then be partly buried and less

(48) Lubini, P.; Zürcher, W.; Egli, M. *Chem. Biol.* **1994**, *1*, 39−45.

(49) (a) Kennard, O.; Cruse, W. B.; Nachman, J.; Prange, T.; Shakked, Z.; Rabinovich, D. *J. Biomol. Struct. Dyn.* **1986**, *3*, 623−647. (b) Westhof, E. *Int. J. Biol. Macromol.* **1987**, *9*, 186−192.

(50) Thibaudeau, C.; Plavec, J.; Garg, N.; Papchikhin, A.; Chattopadhyaya, J. *J. Am. Chem. Soc.* **1994**, *116*, 4038−4043 and cited therein.

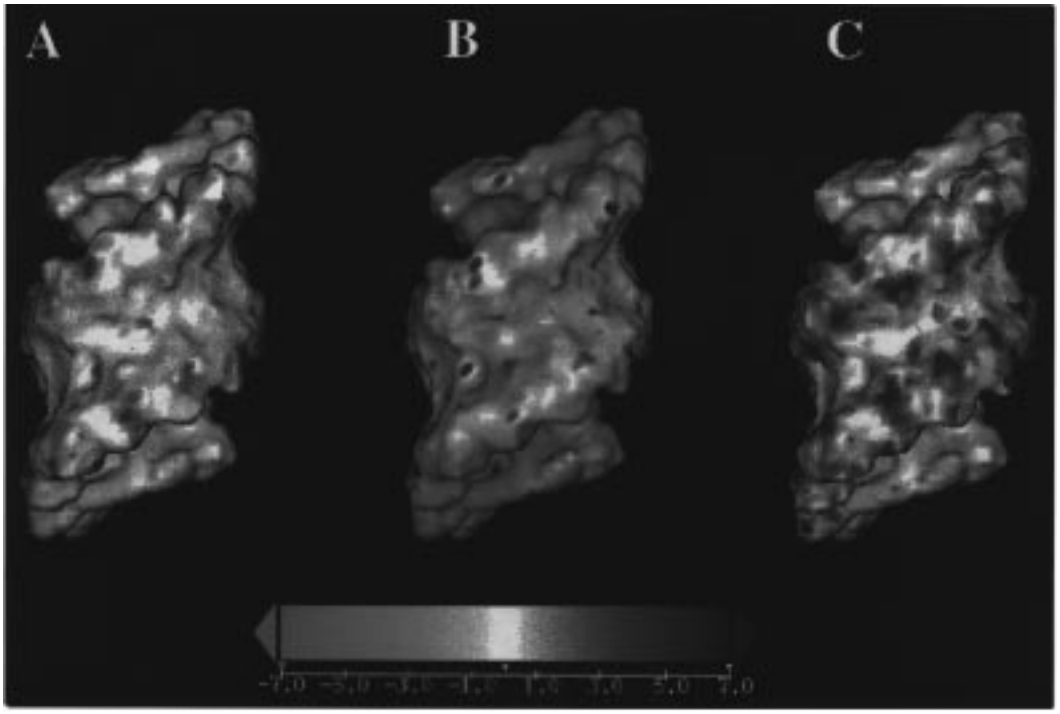

Figure 10. Surface representations of dodecamer duplexes, colored according to electrostatic potential, showing differences in the minor groove and backbone potentials among DNA, 3′-NP DNA, and RNA. (A) Difference in the potentials between 3′-NP DNA and DNA (3′-NP DNA minus DNA). (B) Potential of 3′-NP DNA. (C) Difference in the potentials between 3′-NP DNA and RNA (3′-NP DNA minus RNA). The views are into the minor grooves, blue areas indicate more positive potential, red areas indicate more negative potential, and white areas indicate an intermediate potential range. Note the overall more positive backbone and bordering groove regions in 3′-NP DNA in comparison with both DNA and RNA. The patches of negative potential in (C) indicate the positions of the RNA 2′-hydroxyl groups; the close vicinity between these negative potentials and the positive polarization caused by the 3′-amino groups is clearly visible. The drawings were generated with the program DELPHI in the INSIGHT-II suite, and the overall shapes of the three molecules are identical and based on the structure of the phosphoramidate duplex 1. A partial charge of −0.47 was assigned to the 3′-nitrogen with 3′-NP DNA. The potential scale which was used to produce the individual drawings is shown below the 3′-NP DNA duplex.

accessible to solvation. Molecular dynamics simulations have shown that, in the single-stranded state, both the N3′- and the N5′-modified backbones have comparable solvent-exposed phosphoramidate groups. However, in the duplex form, the solvent accessible surface of the nitrogen in 5′-PN DNA is 10 times less than that of 3′-NP DNA.[22] Taken together, the structural and computational results provide a plausible explanation for the failure of 5′-PN DNA to pair either with itself or with RNA.

Phosphoramidate DNA as an RNA Mimetic. Conclusions. One of the insights which has been gained from several years of experience with oligonucleotide analogues is that improving the RNA affinity of an analogue strand requires that its sugar conformation be shifted toward a northern conformation. This would certainly favor RNA analogues, such as 2′-F- or 2′-O-substituted species, over DNA analogues. Therefore, it is initially surprising that 3′-NP DNA as a DNA analogue displays high RNA affinity besides also showing very stable self-pairing. However, a combination of effects causes the deoxyribose ring of phosporamidate DNA to be locked in a northern conformation, enabling it to pair stably with an RNA strand under formation of an A-type duplex. One of these is the altered gauche effect between the 3′-substituent and O4′ in the sugar which significantly reduces its tendency to adopt a southern pucker and brings about a large percentage of the northern state,[12] preorganizing the phosphoramidate strand for an A-type duplex. Judging from the uniformity of the backbone geometry in the crystal structure, one can consider the phosphoramidate DNA strand to be tightly locked conformationally. We stress that A-type conformation and uniformity are not artifacts of the crystal structure, but are consistent with the CD-spectrum of the 3′-NP DNA dodecamer in solution that is essentially identical with the one obtained for the corresponding A-RNA duplex.[10] While the altered gauche effect may preorganize the phosphoramidate strand for an A-type conformation, a second effect, apparent from the ionic environment of the duplex in the crystal structure and the small geometric variations, namely, the anomeric effect between the nitrogen lone pair and antibonding σ^* orbital from the adjacent P−O5′ bond, may be of no less importance in terms of adoption of the A-form. The relative *ap* orientation of the N3′ lone pair (arranged between the nonbridging negatively charged phosphate oxygens) and P−O5′ bond favors this conjugation and is the reason for the preference of the *−sc, −sc* conformation of the phosphoramidate and was proposed to be operative in phosphodiesters as well.[46] The conformational rigidity of the 3′-NP DNA backbone in the crystal suggests that the anomeric effect is attenuated compared with those between the O5′ and O3′ lone pairs and the P−O3′ and P−O5′ bonds, respectively, in phosphodiesters. It is this force that locks the sugar in the northern conformation through further reducing the gauche effect. It is noteworthy in this context that the isomer that was more completely converted from the B- to the A-geometry in a recent molecular dynamics simulation[51] of the 3′-NP DNA dodecamer duplex ("N3′−H out" in the nomenclature of those authors) is not the one that we observe in our crystal structure. However, a 3′-NP dodecamer duplex with A-form geometry and mixed nitrogen configuration

(51) Cieplak, P.; Cheatham, T. E., III; Kollman, P. A. *J. Am. Chem. Soc.* **1997**, *119*, 6722−6730.

(6 "N3′-H in" and 16 "N3′-H out") remained in the A-form throughout the MD trajectory.

3′-NP DNA shares another property with RNA besides adopting a more or less identical A-type duplex conformation. Unlike DNA, it features a hydrogen bonding donor moiety in its backbone. Just like the 2′-hydroxyl groups of RNA, the amino function of phosphoramidate DNA can act as a donor and as an acceptor of hydrogen bonds. The crystal structure reveals an extensive hydration of the 3′-NP DNA backbone which is likely to contribute to its conformational rigidity. Water bridges across the shallow groove which originate at the 3′-amino positions suggest that, just like the 2′-hydroxyl groups in the case of RNA, the amino groups can serve as bridge heads for structured waters over the groove.[35] One should keep in mind though that the arrangement of the 2′-hydroxyl groups along the borders of the RNA minor groove differs from the locations of the amino groups in 3′-NP DNA. The amino groups are essentially part of the backbone and are somewhat less exposed in comparison with the hydroxyl groups. Since 3′-NP DNA shares so many features with RNA, it is perhaps less surprising then, but nevertheless remarkable, that RNA motifs made of 3′-NP DNA can recruit the RNA-binding proteins with similar efficiency as the parent RNA compounds do.[17] In summary, our crystal structure provides qualitative explanations for the remarkable thermodynamic stability of 3′-NP DNA self-pairing and its high RNA affinity. It proves that N3′ → P5′ phosphoramidate DNA adopts an RNA-like A-form duplex which is conformationally more rigid than the RNA and A-DNA counterparts. The crystallographic results also allow a deeper understanding of the pairing properties of further modified 3′-NP DNAs and explain why 5′-PN DNA is unable to form duplexes with RNA.

Acknowledgment. We thank Mr. Larry DeDionisio, Lynx Therapeutics, Inc., for help with the synthesis and purification of the phosphoramidate dodecamers, Dr. Stefan Pitsch, ETH-Zürich, for communicating the UV-melting temperatures of various pyranosyl-RNA duplexes for stability comparisons with 3′-NP DNA, and Professor Albert Eschenmoser, ETH-Zürich, and Professor Robert L. Letsinger and Professor Wayne F. Anderson, both at Northwestern University, for stimulating discussions. We are indebted to Professor W. David Wilson and Dr. Daoyuan Ding, Georgia State University, for making available to us their results from a high-resolution NMR analysis of the phosphoramidate dodecamer prior to publication. This work was supported by NIH Grant R01 GM-55237 (M.E.).

Supporting Information Available: Table with backbone torsion angles, glycosidic torsion angles, and pseudorotation phase angles for individual nucleotides in all three duplexes (Table S1). ($2F_o - F_c$) omit electron density maps around three further regions of the 3-duplex stack; base pair G4·C21 superimposed on base pair A17$^{\#}$·T8$^{\#}$; base pair C3·G22 superimposed on base pair G16$^{\#}$·C9$^{\#}$, and transitions between duplexes 1 and 2 and duplexes 1$^{\#}$ and 3$^{\#}$ from the symmetry related stack (Figure S1); alternative view of the interaction between phosphoramidate moieties and ammonium and chloride ions in the crystal lattice of the 3′-NP DNA dodecamer (Figure S2), and details of a hydration pattern around the phosphoramidate DNA backbone, whereby two water molecules are bound to the 3′-amino group (Figure S3) (9 pages). See any current masthead page for ordering and Internet access instructions.

JA971962H